



Universität Hamburg

DER FORSCHUNG | DER LEHRE | DER BILDUNG



Master's Thesis – Integrated Climate System
Sciences

**Ecosystem-based Adaptation to future
precipitation impacts in Peru during Coastal-El
Niño events**

Maria Esther Caballero Espejo

Matriculation number: 6885792

Born: 24. August, 1992; in: Huancayo, Peru

School of Integrated Climate System Sciences

Universität Hamburg

Hamburg, 15.01.2019

This thesis has been accepted as a Master Thesis by
the Department Geowissenschaften der Universität
Hamburg

1. Reviewer: Prof. Dr. Johanna Baehr, Institute of Oceanography

2. Reviewer: Prof. Dr. Uwe Schneider, Research Unit Sustainability &
Global Change

For my dear godmother (Nelly), may the energy be always with you.

Abstract

This thesis proposes an interdisciplinary adaptation strategy build upon the regulating services of ecosystems to buffer damages by landslides hazards during future Coastal-El Niño events. The objective is to integrate climate projections, geophysical analyses, and agroeconomic assessment; as support and prerequisite for the design of a meaningful, context-specific and cost-effective adaptation option, providing, in turn, socio-economic benefits. The adaptation proposal consists of El Niño projections' analysis using the outputs of the Max Planck Institute Earth System Model (MPI-ESM) for the RCP 4.5 climate scenario. The resulting simulations are then integrated with geophysical information of mass movement susceptibility provided by the Geological Institute of Peru for a danger analysis. The ecosystem-based adaptation design that includes a combination of different proportions of trees, shrubs, and crops according to the danger intensities, is elaborated using the design parameters of soil bioengineering techniques and the agroforestry slope system. Finally, using the El Niño Adaptation agroeconomic model (ENAAM), the feasibility of the adaptation design in croplands is optimized and evaluated. The projections suggest an increase in the probability of "strong" coastal-El Niño events during the rainy season for the next 50 years (2021-2070) compared to the 1961-2010 period. Unlike past historical events, the associated precipitations are likely to equally affect the northern and southern coast of Peru, as well as, part of sloping areas of the west side of the Andes Cordillera. Those areas indicate high levels of danger as they correspond to susceptible places to mass movements activated by extraordinary rainfall. It is shown that by applying the adaptation design it is possible to decrease the danger levels by 15% in all affected lands. In addition, the agronomic analysis shows that cropland damage during El Niño events can go up to 10% in places with very high danger levels. By adapting croplands to landslides hazards, the danger levels decrease, and so an increase in the welfare can be achieved, depending on the level of side benefits that agroforestry provides, compared to when no protective measures are taken. Despite the limitations, the findings support that interdisciplinary research efforts can support the understanding of impacts and opportunities of climate hazards, and improve the transfer of knowledge from science to practice for successful adaptation strategies by using the benefits of ecosystems.

Contents

Abstract	4
1 Introduction	7
2 Methods	11
2.1 Geographical and economical focus	11
2.2 Climate Analysis	13
2.2.1 Model and dataset	13
2.2.2 Method	13
2.3 Geophysical Analysis	15
2.3.1 Dataset	15
2.3.2 Method	16
2.4 Adaptation design	18
2.4.1 Soil bioengineering techniques	18
2.4.2 Sloping Agricultural Land Technology	19
2.4.3 The proposed ecosystem-based adaptation design	20
2.5 Agroeconomic analysis	22
2.5.1 Vegetation allocation and cropland damage	22
2.5.2 Model description	23
3 Results	25
3.1 Temporal and spatial evolution of El Niño in Peru	25
3.2 Danger Intensity and zones of affectation	30
3.3 Design of the adaptation strategy	34
4 Discussions	38
4.1 Advantages and limitations of the climate analysis	38
4.2 Limitations of the danger analysis	39
4.3 Advantages and limitations of the adaptation design	39
4.4 Limitation of the optimization model	40
5 Conclusions	41
5.1 Outlook	42
References	46
Appendices	47

List of Figures

- 1.1 A sequence of the apparent development of the 2016-17 “Coastal” El Niño event and associated rainfall. Source: NOAA (Galvez, 2017). 8
- 1.2 Structure and overview of the methodological approach of the thesis. 10
- 2.1 Topographic map of the study area, Peru. The presence of the Andes Cordillera that crosses the country from north to south separates the three important climatic areas: coast to the west, mountains to the center, and jungle to the east. 12
- 2.2 Location of El Niño regions 1+2, 3, 4 and 3.4 over the equatorial Pacific. Anomaly of sea surface temperature in March 2017. Image adapted from the National Service of Meteorology and Hydrology of Peru (SENAMHI) website. 14
- 2.3 Diagrammatic representation of vegetation with its various functions. 19
- 2.4 The triangular relationship between, sloping percentage, vertical and horizontal distances of the design of the SALT system. 20
- 2.5 Technical variables to be considered into the design approach: slope angle, vertical and horizontal distances. 21
- 3.1 Cumulative Density Function of ICEN values obtained with the MPI-ESM-MR and observation datasets 26
- 3.2 Frequency of CEN events for historical simulations 1961-2010 (left) and for the RCP 4.5 scenario 2021-2070 (right). 27
- 3.3 Seasonal precipitation during the reference period (1981-2010)(left).Variation of precipitation during CEN events: past events (center) and future events (right). 29
- 3.4 Susceptibility to Mass Movement map at a provincial level. 31
- 3.5 Rain factor based on the intervals of variation of precipitation during future (2021-2070) CEN events. 32
- 3.6 Danger intensity map at a provincial level based on the composition of Mass Movement susceptibility and trigger (rain) factor. 33
- 3.7 Effect of the side benefits in the cropland allocation for adaptation. 35
- 3.8 Effect of adaptation side benefits in the total welfare compared with the no adaptation condition. 36
- 3.9 Map of cropland adaptation sites with a maximum Side Benefit. 37

Chapter 1

Introduction

”Large-scale problems do not require large-scale solutions; they require small-scale solutions within a large-scale framework”.

Fleming

Up to now, the increase of climate extremes has served as a proof of an ongoing change in the global Earth System, and it is thought that its large-scale components might reach a critical tipping point that can result in a major climate shift with larger impacts in vulnerable environments (Ove Hoegh-Guldberg et al., 2018). El Niño-Southern Oscillation (ENSO), probably most significant of those large-scale components, is characterized by an ocean-atmospheric coupling that produces deep changes in the global circulation patterns (Cane, 2005; Lenton et al., 2009). It is best known for the effects of its warm phase, El Niño, which leads to warmer-than-average sea-surface and atmospheric temperatures in the eastern Pacific region (e.g. French and Mechler, 2017). Despite being well known due to its widely-spread impacts all over the globe, its effects were first observed by ancient fishing communities in the north coastal area of Peru (e.g. Cane, 2005; French and Mechler, 2017; Lagos et al., 2008).

In 1578, the presence of an intense ocean warming accompanied by heavy precipitations in the normally arid west flank of the Andes Cordillera was characterized as the first mega El Niño on record in Peru. That event showed dramatic damages triggered by the combination of heavy precipitations and unstable terrains (INDECI et al., 2017). Since then, 8 events of an extraordinary intensity were recorded (INDECI et al., 2017; INDECI, 2017), including the last one in 2016-17 (figure 1.2) which emerged almost twenty years after the historic global El Niño phenomenon in 1997-98. This last event started with the occurrence of torrential rains that began in the fourth week of December 2016 and lasted until May 2017. The rapid and local development of this particular “Coastal” El Niño caused floods, landslides, storms, as well as the occurrence of other emergency events and various socioeconomic damages (INDECI, 2017).

Although as described, the frequency of El Niño events of an extraordinary magnitude heretofore is rather low, recent studies indicate that such frequency would increase linearly with the global average temperature (e.g. Ove Hoegh-Guldberg et al., 2018; Cane, 2005). This suggests that the number of extraordinary El Niño events could double in the future entailing, in addition to other consequences, to intensified and more frequent extreme phenomena that imply the greater occurrence of intense rains, droughts, and heat waves in the country (Ministerio del Medio Ambiente del Perú, 2016).

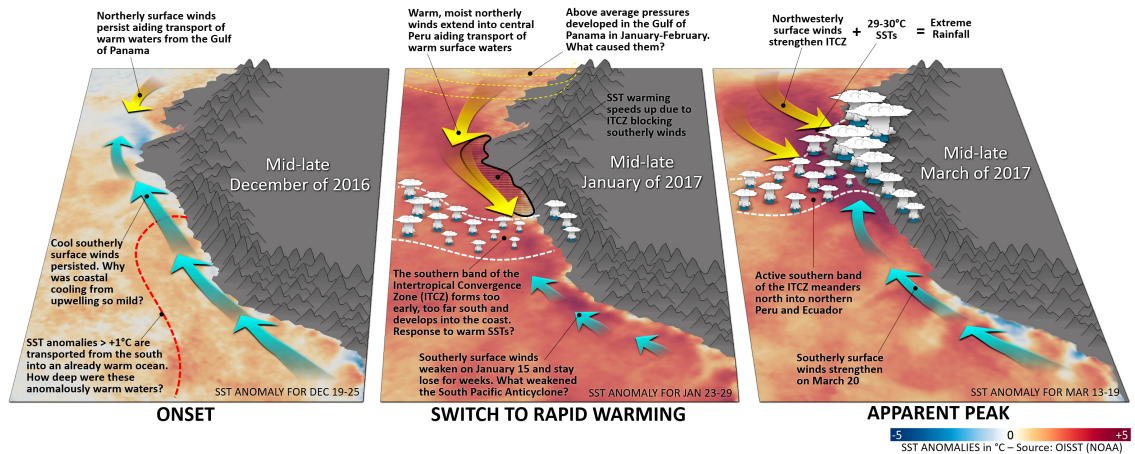


Figure 1.1: A sequence of the apparent development of the 2016-17 “Coastal” El Niño event and associated rainfall. Source: NOAA (Galvez, 2017).

Alongside, Peru is also exposed to dangers generated by external geodynamic phenomena, such as mass movements, due to the relief of the territory and the current high deforestation process (INDECI, 2017). These effects place Peru as one of the most vulnerable countries in the world, because the interaction between meteorological phenomena and the physical, ecological and demographic configuration of its territory can exacerbate the conditions of poverty and inequality in vulnerable ecosystems of global importance (Damonte et al., 2018; Ministerio del Medio Ambiente del Perú, 2016).

Therefore, given the combination of factors that demonstrate that the level of risk to disasters is high, it is necessary to increase the resilience of communities. That is the reason why as part of the disaster risk management, climate adaptation is a very crucial process that includes the planning and implementation of measures to prevent, moderate, cope with and take advantage of climatic perturbations and their effects (Damonte et al., 2018; Johnson and Krishnamurthy, 2010; Zölch, 2017).

The situation in Peru in regard to adaptation; however, calls into question the country’s ability to learn from its own lessons and experiences. The last El Niño phenomenon reiterates the problem of the big disasters that have occurred in the country during the last 20 years. Despite the significant advances in adaptation as a result of the integration of the concepts of risk management and climate change in the instruments of planning and investment (Canales et al., 2014; Damonte et al., 2018). What happened in 2017 showed again similar socio-economic losses as the previous events and more than 40% of structural damages due to the practically nonexistent territorial management capacities for preparedness (Damonte et al., 2018; Galarza et al., 2012; INDECI, 2017).

Current preparation activities to climate extremes in Peru show that the majority of adaptation projects have often been implemented with a sectoral perspective, without sufficient physical and social information, and without taking into account the territorial reality in which they operate (Damonte et al., 2018). A more detail analysis in the subject shows that in terms of planning it is evident that the prevention plans focus more on the response and less on the preparation. In the face of threats such as the impacts of El Niño, preventive measures are summarized in the widening of riverbeds, protection of river borders and cleaning of drainages (Galarza et al., 2012). In addition, the risk scenarios that should constitute the framework for contingency planning are designed based on past climatic events, considering stable zones of af-

fection and without including recurrent hazards -such as heavy rains and landslides (INDECI, 2017; Niño-Zarazúa et al., 2012; Sabates-Wheeler and Devereux, 2010).

On the other hand, the importance of science and climate information in supporting management of the risk to disasters allows identifying certain opportunities in the generation of physical and social information for the implementation of adaptation projects. Presently, climate adaptation takes various forms of applied actions going from hard approaches which refer to engineering measures designed to withstand climatic variability and extremes, and soft measures that encourage adaptive behavior by, for example, providing information and incentives (Zölch, 2017). Although these measures can create a great impact by themselves, the adaptation of a system has to be seen as an active process that requires an integral vision in its design and application to respond to the effects of hazards as a function of the territory.

While, in the particular case of Peru, some studies have been done on disaster risk scenarios to the occurrence of El Niño events (e.g. CENEPRED, 2012; Ministerio del Medio Ambiente del Perú, 2015; INDECI, 2016) to support the preparations measures taken, there are a number of gaps in terms of multidisciplinary that need to be filled. For instance, the necessity for developing feasible preparation strategies fitting the biophysical and social reality in the face of future El Niño impacts incorporating adequate climate information. Hence, in this thesis, we propose a comprehensive and tailored adaptation strategy that begins with a climate analysis, i.e. evaluate future states of El Niño and related hazards, to then incorporate that information into the design of a preventive plan adapted to the livelihoods of the most affected communities. In order to approach that aim, the following research questions are to be answered:

- **Which future El Niño changes can be expected, given the development in the recent past? Is the suggested increase in number and intensity of future El Niño events and impacts detected?**
- **If so, how can that information be included to design an adaptation plan to El Niño impacts?**
- **Consequently, which adaptation option for the most recurrent hazard is the most suitable, feasible and cost-effective environmentally, geographically and socioeconomically speaking?**

The outcomes achieved from the translation of scientific information into the designing of adaptation measures are meant to be used as recommendations for decision-making and implementation of adaptation options. Additionally, it is intended for this methodology to be a model of adaptation planning.

The structure of this thesis has started by revising the disaster risk management and current adaptation measures of the Peruvian government. The findings support the design of the methodology in chapter 2, which integrates climate projections, geophysical analyses, and agroeconomic assessment; as support and prerequisite for the design of a meaningful, context-specific and cost-effective adaptation option. This chapter supports the argument that an integral adaptation design can contribute to the mitigation of hazards. The results are then discussed in terms of the future expected changes in El Niño impacts, and the synergies and multifunctional benefits of the adaptation design in chapter 3. Practical implications for the implementation of the methodology in adaptation planning are derived in chapter 4 as part of the general discussions. Finally, the overall conclusions are presented in chapter 5. Figure 1.2 illustrates the approach.

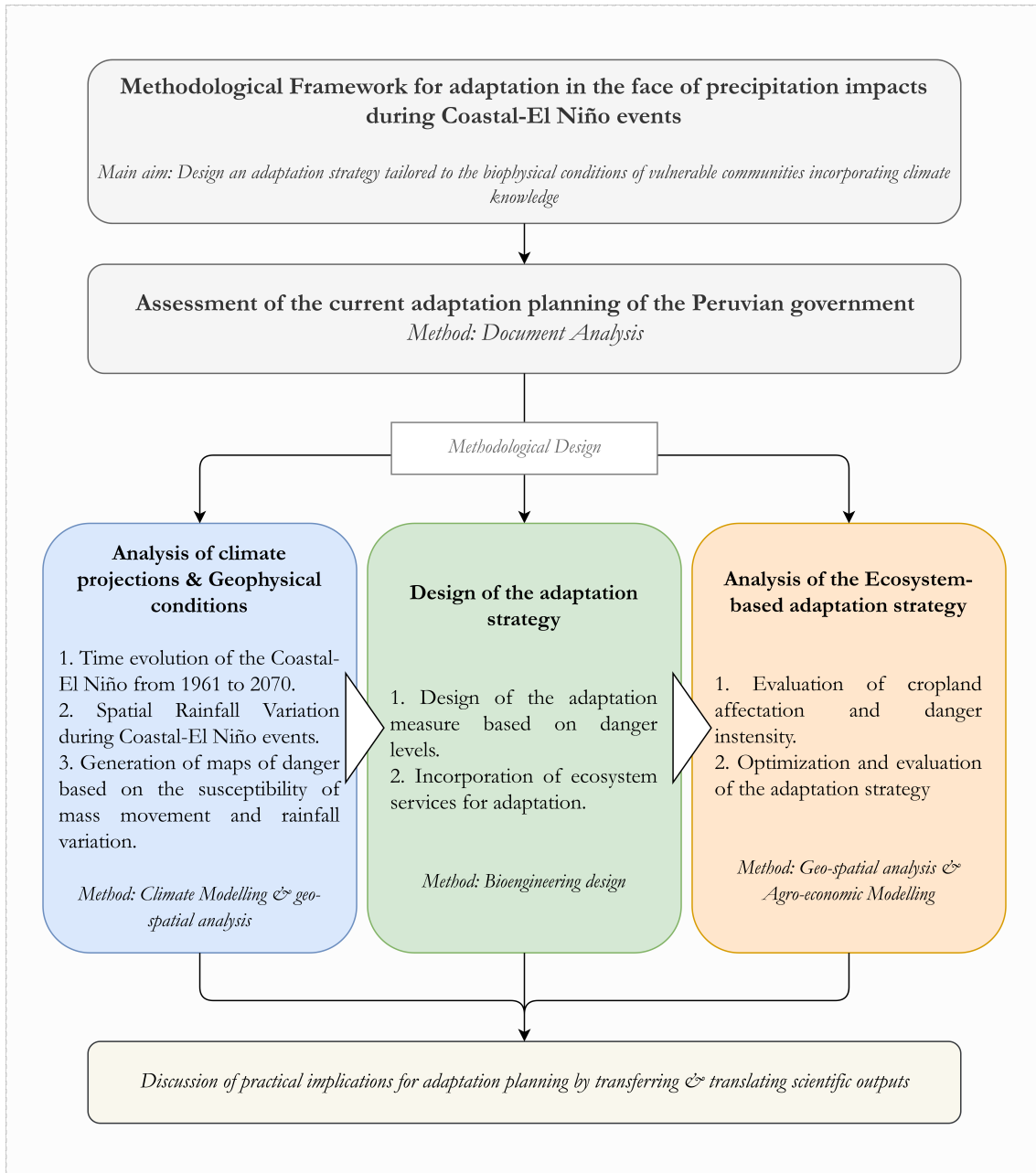


Figure 1.2: Structure and overview of the methodological approach of the thesis.

Chapter 2

Methods

To approach the research questions, this chapter is broken down into five sections. The first section is intended to provide a brief geographical and economical focus of the study area. Then, in the following sections, we detail the data and methodologies used for: the analysis of El Niño states in the past and the future, and related effects; the translation of that analysis for the identification of places in danger; to finally, design, and evaluate the adaptation measure.

2.1 Geographical and economical focus

Peru is geographically located in the central western part of South America just underneath the Equatorial line. It is also a highly heterogeneous country due to the confluence of two ocean currents of different characteristics and the presence of the Andes Mountains, which divide the country into three major important climatic zones with different topographic conditions (figure 2.1). The arid coast in the west flank, the mountain areas in the middle and the tropical rainforest that provides humidity to the east flank of the Andes, in the east (SENAMHI, 2009). From the perspective of multiannual variation of extreme temperatures and precipitation, they respond to the geographic conditions previously described but are also determined by the occurrence of ENSO.

In economic terms, Peru is a country with great natural economic resources, typical of its geographical configuration. Thanks to this wealth, mining represents one of the most important economic sectors in Peru. As well as agriculture that has become one of the main economic activities that drive economic development. Moreover, in recent years, Peru has become one of the ten largest food suppliers in the world (Lampadia, 2015).



Figure 2.1: Topographic map of the study area, Peru. The presence of the Andes Cordillera that crosses the country from north to south separates the three important climatic areas: coast to the west, mountains to the center, and jungle to the east.

2.2 Climate Analysis

The first step to analyze El Niño and related effects in Peru is to determine the appropriate El Niño study region (see figure 2.2). At the global level, the majority of prediction centres monitor El Niño inspecting changes in the Tropical Central Pacific, better known as El Niño 3.4. This region has a closer relationship with the atmospheric fluctuations of ENSO and with climatic alterations at a global level (Martínez and Takahashi, 2017). Nevertheless, for the local effects, the multisectoral committee in charge of the National study of El Niño Phenomenon in Peru (ENFEN in Spanish) has developed a more relevant index to the South American coast that allows determining objectively the presence of El Niño or La Niña and their magnitudes (Takahashi et al., 2014). That is, the Coastal-El Niño index (ICEN in Spanish) based on the three-month running average of the monthly anomalies of SST in El Niño 1+2 region (90°W - 80°W, 10°S - 0°), taking the reference period from 1981 to 2010 (ENFEN, 2012; Takahashi et al., 2014).

2.2.1 Model and dataset

For the calculations to proceed, we use the dataset from the Earth System Model at mixed resolution developed at the Max Planck Institute for Meteorology: MPI-ESM-MR. This model combines the major components of the climate system, and it is employed to simulate the historical climate and its behaviour in the future taking the Representative Concentration Pathway (RCP) scenarios. The atmospheric and land components of the MPI-ESM-MR use a horizontal grid representing a resolution of 1.9°; while the ocean component offers a horizontal grid spacing of 0.4° (see Giorgetta et al., 2013). For the purposes of this study, the period of 1961-2010 is used for the analysis of the past El Niño events, and the period of 2021-2070 for the future events following the RCP 4.5 scenario. The latter is employed because it assumes that climate policies are invoked to achieve the goal of limiting emissions and radiative forcing at 4.5 $W.m^{-2}$.

Since the ENFEN uses the Extended Reconstructed Sea Surface Temperature (ERSST) dataset produced on a 2° horizontal grid, derived from the International Comprehensive Ocean-Atmosphere Dataset (ICOADS) for the monthly calculation of the ICEN. This product is included likewise.

2.2.2 Method

Once El Niño 1+2 has been identified as the study region, is it important to bear in mind that the different thresholds used for the definition of the ICEN magnitudes (table 2.1) are set based on observations. Therefore, an adjustment of the model (MPI-ESM-MR) ICEN values to the ICEN categories established by the ENFEN has to be made. To do so, we calculate the probability distribution and other statistical values (quantiles, mean, and max) of the determined ICEN values by both datasets, using the Cumulative Distribution Function (CDF). The calculation of the CDFs given in the equation (2.1) is rather a simple approach to find out the model-based ICEN categories' thresholds that are compared to the operational categories.

$$F(x) = P(X_{ICEN} \leq x) \quad (2.1)$$

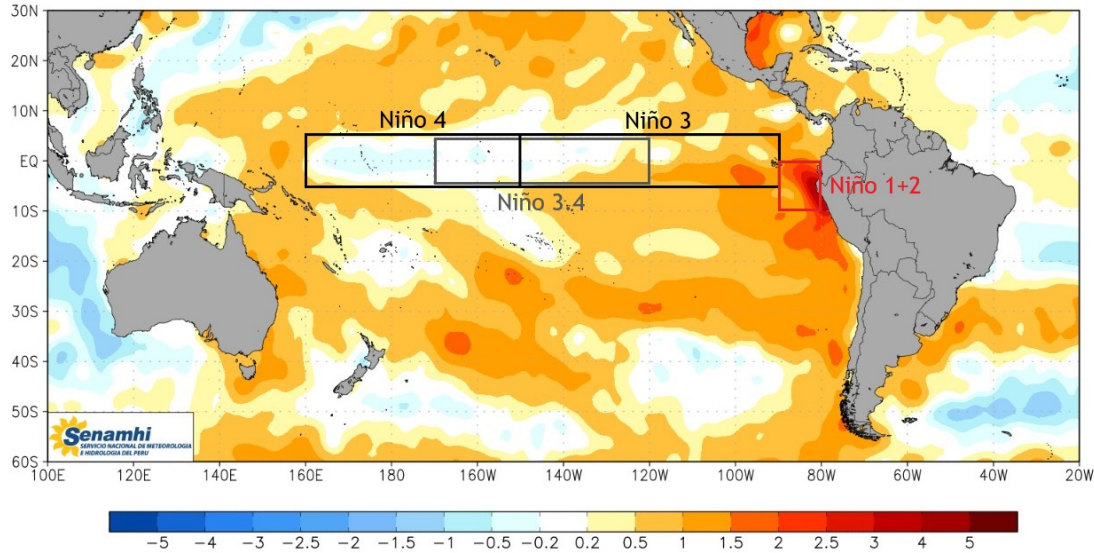


Figure 2.2: Location of El Niño regions 1+2, 3, 4 and 3.4 over the equatorial Pacific. Anomaly of sea surface temperature in March 2017. Image adapted from the National Service of Meteorology and Hydrology of Peru (SENAMHI) website.

Table 2.1: Categories of anomalies in the conditions of the temperature according to ICEN. Source: ENFEN, 2012.

Categories	Monthly value of ICEN
Strong-Cold	<i>Less than -1.4</i>
Moderate-Cold	<i>Greater than or equal to -1.4 and less than -1.2</i>
Weak-Cold	<i>Greater than or equal to -1.2 and less than -1.0</i>
Neutral	<i>Greater than or equal to -1.0 and less than or equal to 0.4</i>
Weak-Warm	<i>Greater than 0.4 and less than or equal to 1.0</i>
Moderate-Warm	<i>Greater than 1.0 and less than or equal to 1.7</i>
Strong-Warm	<i>Greater than 1.7 and less than or equal to 3.0</i>
Extraordinary-Warm	<i>Greater than 3.0</i>

With the definition of the ICEN categories for the model, we now follow the identification approach of the Coastal-El Niño (CEN) events in the two study periods. The ENFEN states that a CEN event is detected when the ICEN shows “warm conditions” lasting for at least three consecutive months. For the purpose of the study, only “strong” and “extraordinary” categories are considered because of their significance at triggering hazardous rains.

The strong and extraordinary CEN events in Peru cause a greater presence of precipitation, in the otherwise arid coast, associated with the development of deep convection triggered by the accumulation of anomalously warm waters in the region (Lavado and Espinoza, 2014). This situation as recorded in previous extraordinary events gives rise to landslides and floods (INDECI, 2016). Hence, given that precipitation is an essential variable to recognize the impacts of El Niño, and taking into account that these impacts are exacerbated during the rainy season. CEN-related effects can be interpreted as the percentage variation in precipitation (VP_{CEN}). This is obtained by calculating the difference of the maximum value of precipitation in a CEN event ($MaxPP_{CEN}$) with respect to the maximum mean precipitation value in the reference period ($MaxPP_c$) during the rainy season:

$$VP_{CEN} = (MaxPP_{CEN} - MaxPP_c * 100) / MaxPP_c \quad (2.2)$$

The resulting variations in rainfall in each identified event serve to compose maps for each sub-season (SON, DJF, and MAM) within the rainy season to better evaluate the correct representation of the model with respect to the distribution of normal precipitation and its variation when CEN events take place.

2.3 Geophysical Analysis

The above climate analysis is incorporated in this section, which determines the level of danger to hazardous CEN impacts, by merging the variation of precipitation during “strong” and “extraordinary” CEN events with the susceptibility to mass movement information of the country.

In previously recorded El Niño events, the mud avalanches, or “huaicos” (in quechua language), occurred continuously. They affected roads and basic services and with it the supply of food in some areas. In addition, the damage to agriculture and food security resulted in the loss of several thousand hectares of crops and an increase in acute malnutrition (INDECI, 2017). This overall situation tells about the severe threat to infrastructure, agricultural land, and even human life, landslides pose in Peru. Topographic, geomorphological and hydrological features are seen as primary factors controlling landslide susceptibility (Moos, 2014). In Peru, the particular geographical situation due to the presence of the Andes Cordillera conditions a perfect scenario for the development of mass movement phenomena.

2.3.1 Dataset

This section of the analysis uses geographical information compiled from the Geological Institute of Peru (INGEMET in Spanish). They have created the map of “Susceptibility to Mass Movement”, with a horizontal resolution of 100 m^2 . The objective of the map is to propose a model that indicates the areas with the greatest propensity to mass movements in the territory. Equation (2.3) shows the usage of cartographic data

where the topographic, geomorphological, lithological, structural, vegetation cover and land uses, as conditioning factors, are analyzed and expressed in the following:

$$SMM = (SVC(0.05) + SHG(0.1) + SGM(0.25) + SP(0.2) + SL(0.4))/5 \quad (2.3)$$

Here, the susceptibility level (SMM) is given by the incorporation of the susceptibility by: vegetation cover (SVC), hydrogeology (SHG), geomorphology (SGM), slope (SP), and lithology (SL) (Villacorta et al., 2015).

2.3.2 Method

The approach applied arose from a combination of techniques and methods for the integration of the future CEN events information into the determination of places in danger. The landslides danger levels owing the occurrence of heavy rains during CEN events are determined by a multicriteria analysis suggested by the United Nations Development Programme (UNDP) (PNUD Cuba, 2014), which seeks to answer three questions:

- Where the event will occur?
- When the event will occur? And,
- How the event will happen?

To answer the first question, we rely on the susceptibility map of INGEMET that considers five levels of susceptibility (table 2.2) having as "triggers" the intense rainfall. This map is reproduced at the province level to standardize our spatial resolution.

The next question is addressed by determining the probability of occurrence of CEN events of "strong" and "extraordinary" intensity, and its respective return period. Using the equation (2.4), the probability of occurrence of a CEN event during a sub-season (F_{CEN}) is calculated based on the number of future CEN events identified per each sub-season (n_{CEN}) and the total number of sub-seasons (ss) in the future (2021-2070).

$$F_{CEN} = 100 * (2n_{CEN} - 1)/2ss \quad (2.4)$$

Further, the return period is given by:

$$R_{CEN} = 1/F_{CEN} \quad (2.5)$$

Lastly, to address the third question we determine the intensity levels of landslides danger during CEN events. The intensity danger level (DI) is a function of the susceptibility factor (SF), and the intensity of rainfall caused by CEN events, i.e., the rain factor (RF).

$$DI = f(SF; RF) \quad (2.6)$$

The susceptibility factors are already given by the susceptibility levels. Then, for the calculation of the rain factor, the maps of the VP_{CEN} generated following the methodology of the previous section are used. With these results, a division into five intervals of VP_{CEN} is made for each province, taking a minimum and a maximum

Table 2.2: Mass Movement Susceptibility levels in Peru. Source: INGEMET, 2015.











Level	Description
 Very High	<i>Slopes with fault zones, rock masses intensely weathered, saturated and very fractured. Slopes between 30° to 45°, internal and/or old mass movements. In these sectors, there is a high possibility of mass movements occurrence.</i>
 High	<i>Slopes that have fault zones, rock masses with high to moderate weathering, fractured with unfavorable discontinuities. Slopes between 25° and 45°, where mass movements have occurred or are likely to occur.</i>
 Medium	<i>Slopes with some fault zones, intense erosion or partially saturated materials, moderately weathered, slopes with slopes between 20° and 30°. These can be "detonated" by earthquakes and exceptional rains.</i>
 Low	<i>Slopes with slightly fractured materials, moderate to little weathering, partially eroded. Slopes between 10° to 20°. Areas that have few conditions to originate mass movements.</i>
 Very Low	<i>Slopes not weathered. Land with slopes lower than 5° where there are no indications to predict landslides.</i>

Table 2.3: Rain factor levels established in relation of the variation of precipitation during future CEN events.

Rain Factor	Variation of pp (%)
 1	55 - 85
 2	86 - 155
 3	156 - 275
 4	276 - 405
 5	406 - 600

percentage variation of precipitation in the territory. This division can be seen in table 2.3.

For the danger level mapping, we use the geographical information system ArcGIS in its 10.3 version. The susceptibility factor and the trigger factor layers are combined here, resulting from that the following intervals, in table 2.4, for the classification of the intensity of danger.

Table 2.4: Danger matrix determined by the rain factor and susceptibility levels.

Rain factor	5	5	10	15	20	25
	4	4	8	12	16	20
	3	3	6	9	12	15
	2	2	4	6	8	10
	1	1	2	3	4	5
		<i>Very Low</i>	<i>Low</i>	<i>Medium</i>	<i>High</i>	<i>Very High</i>
		Susceptibility level				

2.4 Adaptation design

By extending the focus beyond conventional technical solutions that, focus the problem of withstanding landslides by the usage of grey structures. The opportunity to incorporate natural-based adaptation measures become more appealing due to the resilient role of ecosystems and their added socio-economic benefits in a country with high biodiversity such as Peru. Measures to achieve an integrated danger management include, e.g., ecological restoration, wetland and floodplain conservation, afforestation and reforestation, ecological corridors, soil bioengineering techniques, agroforestry, and others (Grizzetti et al., 2016; Arkema et al., 2017).

In the following, we present two design approaches and the very own adaptation proposal for reducing the danger to landslides. All of them are supported in ecosystem services (ES) which act as regulators that reduce the instability of soils caused by extremes rainfall events (Martinez-Alonso et al., 2010).

2.4.1 Soil bioengineering techniques

Bioengineering is the application of engineering design and technology to living systems. In the context of upland slope protection and erosion reduction, combines mechanical, biological, and ecological concepts to arrest and prevent erosion and shallow landslides, stabilizing slopes using vegetation (see Bobrowski, 1997; Shrestha et al., 2012; US Department of Agriculture Natural resource Conservation service, 1992). It is most suitable to be deployed in developing countries because of their cost-effectiveness and environmentally friendly nature (Raut and Gudmestad, 2017).

Among the benefits given by plants for soil stabilization, the mechanical and hydrological functions can be highlighted (figure 2.3). The first one lays on the fact that roots form a network-like structure underneath the ground that binds and anchors the soil increasing the shear strength. The second involves the removal of soil water by evapotranspiration through vegetation. It increases ground suction which ultimately increases the shear strength of the soil (Bischetti et al., 2010; Raut and Gudmestad, 2017).

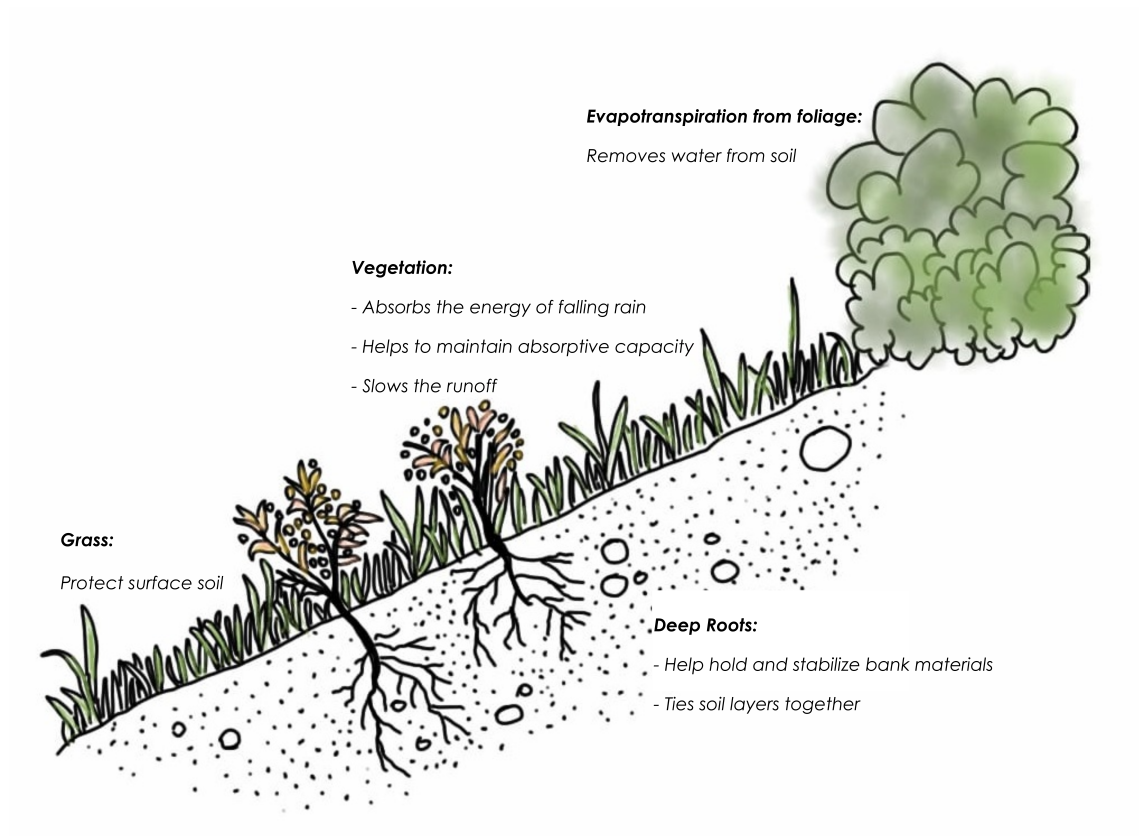


Figure 2.3: Diagrammatic representation of vegetation with its various functions.

In soil bioengineering, there are minimum requirements to be considered for its implementation such as the spacing between vegetation species and the minimum coverage of trees. For the adaptation proposal, we make a use of the relationship between the sloping angle and the spacing of trenches indicated in table 2.5. Additionally, the minimum tree coverage of around 40% is included as a condition, for the most dangerous locations (US Department of Agriculture Natural resource Conservation service, 1992).

Table 2.5: Relationship between the slope angle and trenches spacing. Source: US Department of Agriculture Natural resource Conservation service (1992)

Slope angle (°)	Distance between trenches (cm)
45 - 35	91 - 121
35 - 30	121 - 152
30 - 25	152 - 182
25 - 18	182 - 243
18 - 15	243 - 274
15 - 11	274 - 304

2.4.2 Sloping Agricultural Land Technology

This system, commonly known as SALT, is an Agroforestry scheme developed in Davao del Sur by the Mindanao Baptist Rural Life Center. It employs contour terraces for the improvement of soil structure, fertility, and enhancement of food crop production

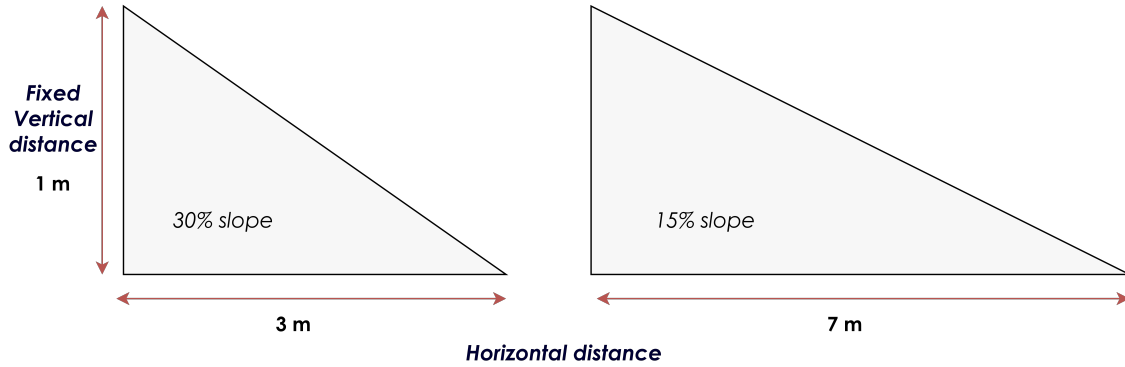


Figure 2.4: The triangular relationship between, sloping percentage, vertical and horizontal distances of the design of the SALT system.

while being economically feasible (Tej and Harold, 1994). The technique forms the basis of “conservation agriculture with trees” in sloping areas (Roshetko JM, Mercado Jr AR, Martini E, 2017).

The technical design of this system suggests taking the mountainous slopes as rectangular triangles, such as those shown in figure 2.4. There, for a fixed vertical distance, the consequent horizontal distance depends on the slope percentage.

2.4.3 The proposed ecosystem-based adaptation design

In order to apply the approaches already described, we develop an ecosystem-based adaptation (EbA) system that responds to each level of landslides danger. The design considered here employs the following variables: slope angle (Sa), slope percentage (Sp), vertical distance (VD), horizontal distance-A (HD_A), and horizontal distance-B (HD_B), which are illustrated in Figure 2.5. They are determined based on the estimated slope values for each level of susceptibility (see table 2.2). From this, a relationship is established between the slopes and distances, so that the following equations can be formed:

$$VD = 0.02 * Sp + 0.525 \quad (2.7)$$

$$HD_A = VD / \sin(Sa) \quad (2.8)$$

The horizontal distance-B does not depend on the slope but on the vegetation cover, i.e., the percentage of the type of vegetation allocated for each level of danger. Then, following the recommendations of the soil bioengineering technique, a minimum spacing of 2 meters is considered for major plant species, e.g. trees.

Ultimately, based on the technical aspects described by these variables and danger levels, the allocation of three plant species: trees, shrubs and crops in a crop field is determined (see Appendix A).

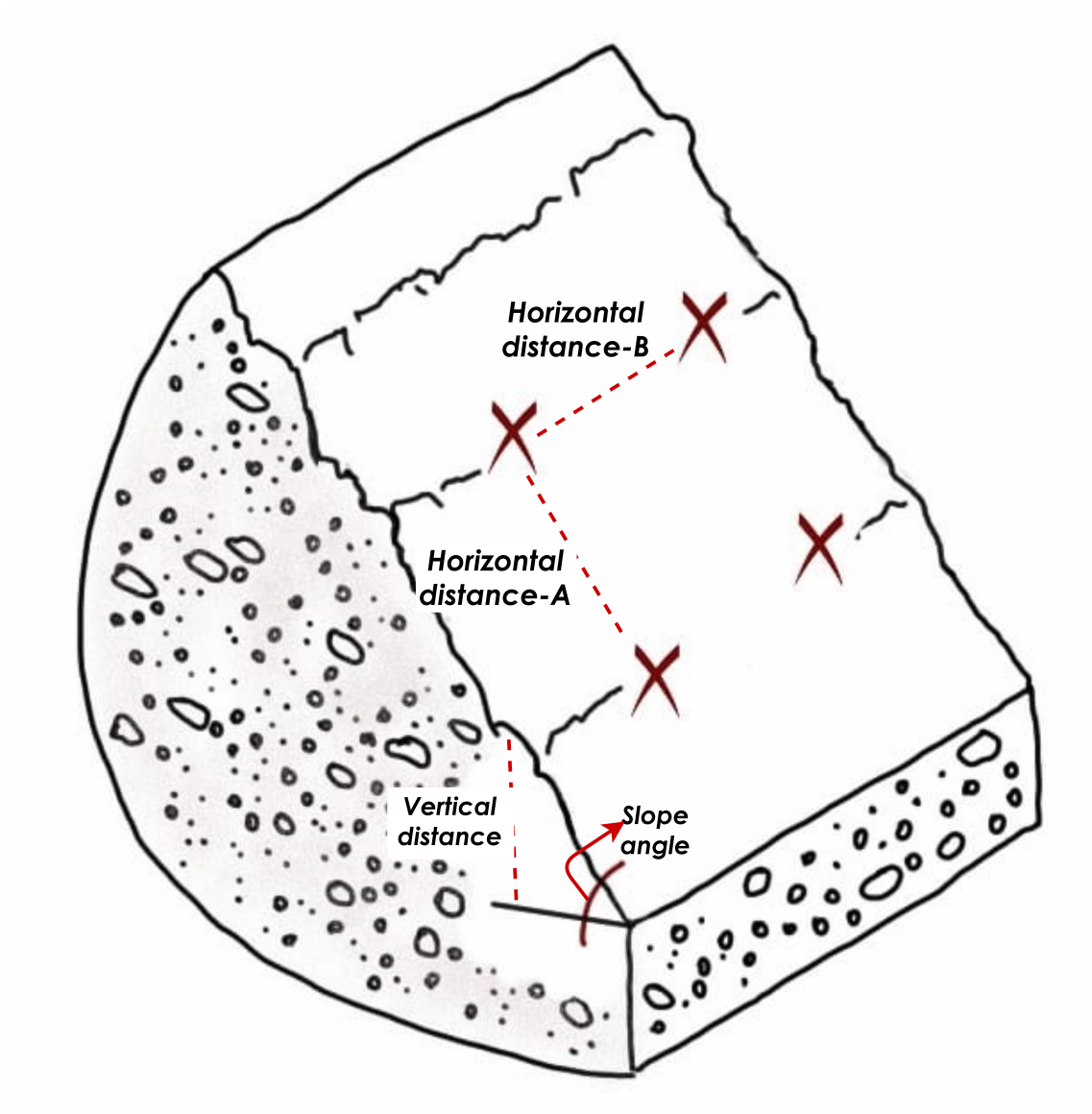


Figure 2.5: Technical variables to be considered into the design approach: slope angle, vertical and horizontal distances.

2.5 Agroecconomic analysis

To assess the economic feasibility of the adaptation design, we make an agroecconomic analysis by using El Niño-Adaptation Agroecconomic Model (ENAAM), which is a mathematical optimization model written in the General Algebraic Modeling System (GAMS). ENAAM covers the period from 2021 to 2070, the crop and spatial resolutions account for a group of 12 crop types and 195 provinces, which form part of the 25 political regions of Peru (See table 2.6). In addition, the land quality classes assigned as homogeneous response units (HRU) are based on differences in altitude, soil texture, and slope; for the country, we use 4328 simulation units. The objective function of ENAAM simulates the national surplus obtained by agricultural activities by maximizing the welfare over all provinces and vegetation types included for adaptation subject to restrictions by resource allocation, cropland damage, side adaptation benefits, and for a given probability of occurrence of “Strong” El Niño events in the period 2021-2070.

Table 2.6: Scope and resolution of the El Niño-Adaptation Agroecconomic Model (ENAAM).

Regions		Crop types
Lambayeque	Amazonas	Corn
Lima	Ancash	Rice
Lima Metropolitana	Apurimac	Sorghum
Loreto	Arequipa	Barley
Madre de Dios	Ayacucho	Potatoes
Moquegua	Cajamarca	Cassava
Pasco	Callao	Sweet potatoes
Piura	Cusco	Drybeans
Puno	Huancavelica	Chickpeas
San Martin	Huanuco	Sugar Cane
Tacna	Ica	Soy beans
Tumbes	Junin	Peanuts
Ucayali	La Libertad	

To set up the model to the specific agricultural conditions of the country. The crop yields for different management options, soil textures, altitudes, slopes, and climate zones are derived from the Environmental Policy Integrated climate (EPIC) model (see Gassman et al., 2005). This information is then calibrated using as references the national averages on yields, harvested areas, prices, and production of the historical crop data for traditional products from the FAOSTAT (FAO (Food and Agricultural Organization of the United Nations), 2018) database.

2.5.1 Vegetation allocation and cropland damage

ENAAM is meant to solve a decision problem deciding when is economically suitable to apply the adaptation technology describe as the allocation of vegetation types, i.e. trees, shrubs and crops, according to the percentage of agricultural damage associated to each danger level calculated using the Coastal-El Niño 2016-17 reports of affectation

from INDECI et al. (2017), side benefits of adaptation stripes, and the probability of CEN occurrence.

2.5.2 Model description

Table 2.7 includes all the sets, parameters and variables used in the model.

Table 2.7: Description of ENAAM sets (a), parameters (b), & variables (c).

a)

Symbol	Description
c	All crops: cassava, corn, rice, sorghum, soybeans, sugarcane, dry-beans, potatoes, sweet-potatoes, chickpeas, barley, peanuts Non crop vegetation: forest & shrubs
a	Adaptation technology: none, crop_adaptation
s	Nature state: El Niño, Normal
r	Studied region: 198 provinces, 25 regions
t	Studied period: 2020 to 2070
m	Management system: irrigation, fertilization
p	Products: cassava, corn, rice, sorghum, soybeans, sugarcane, dry-beans, potatoes, sweet-potatoes, chickpeas, barley, peanuts

b)

Symbol	Domain	Unit	Description
U	t,r,s	1000 ha	Resource endowment (Cropland or Total arable land)
u	r,a,s	ha/ha	Unit resource per hectare
γ	t,r,c,m,a,s,p	tons/ha	Crop yield
c	t,r,c,m,a,s	USD/ha	Unit cost of producing a crop
b	r,a	USD/ha	Side Benefit of non-crop species
z	t,r	USD/ha	Unit cost of land resource
P	-	USD/ton	Market prices
ρ	t,s	%	Probability of occurrence

c)

Symbol	Domain	Unit	Description
Q	t,p,s	1000 tons	Product demand
A	t,r,s	1000 ha	Adaptation activity
L	t,r,c,m,a,s	1000 ha	Level crop activity
W	t,s	1000 USD	Total economic surplus

In ENAAM all the variables are non-negative, except for the objective function shown in equation (2.9). This equation sums up the product of welfare ($W_{t,s}$) and the probability of nature states ($\rho_{t,s}$).

$$Max \sum_{t,s} \rho_{t,s} \cdot W_{t,s} \quad (2.9)$$

Equation (2.10) represents the welfare obtained by summing up the product of consumption (Q) and market prices (P). To which we add the additional benefits of non-crop vegetation types used for adaptation ($b_{r,a} \cdot L_{t,r,c,m,a,s}$); minus the costs of giving up cropland for their establishment ($c_{t,r,c,m,a,s} \cdot L_{t,r,c,m,a,s}$), the costs of implementation of the adaptation technology ($c_{t,r} \cdot A_{t,r,s,"new"}$), and the land resource costs ($z_{t,r} \cdot U_{t,r,s}$).

$$W_{t,s} = \left\{ \begin{array}{l} + \sum_p \int_{\tilde{q}}^{Q^*} P \cdot (Q_{t,p,s}) dQ_{t,p,s} \\ + \sum_{r,c,m,a} ((b_{r,a} - c_{t,r,c,m,a,s}) \cdot L_{t,r,c,m,a,s}) \\ - \sum_r (z_{t,r} \cdot U_{t,r,s}) \\ - \sum_r (c_{t,r} \cdot A_{t,r,s,"new"}) \end{array} \right\} \forall t, s \quad (2.10)$$

The model constraints are given by equation (2.11), which ensures that consumption ($Q_{t,p,s}$) does not exceed the sum of production ($\gamma_{t,r,c,m,a,s,p} \cdot L_{t,r,c,m,a,s}$):

$$Q_{t,p,s} - \sum_{r,c,m,a} (\gamma_{t,r,c,m,a,s,p} \cdot L_{t,r,c,m,a,s}) \leq 0; \quad \forall t, s, p \quad (2.11)$$

The adaptation equation (2.12) establishes a dynamic module for new adaptation, meaning that the total adaptation (A) expands each time:

$$A_{t,r,s,"total"} = A_{t-1,r,s,"total"} + A_{t,r,s,"new"}; \quad \forall t, r, s \quad (2.12)$$

Equation (2.13) is the equation for adaptation limit, which forces the activity levels ($L_{t,r,c,m,a,s}$) to fall within the total adaptation (A):

$$\sum_{c,m,a} L_{t,r,c,m,a,s} \leq A_{t,r,s}; \quad \forall t, r, s \quad (2.13)$$

The resource constraint is given by equation (2.14). Here the availability of arable land restrict agricultural activities. The sum product of unit resource use ($u_{r,a,s}$) and activity level ($L_{t,r,c,m,a,s}$) may not exceed the resource endowments ($U_{t,r,s}$):

$$\sum_{c,m,a} (u_{r,a,s} \cdot L_{t,r,c,m,a,s}) - U_{t,r,s} \leq 0; \quad \forall t, r, s \quad (2.14)$$

Finally, the resource limit is given by:

$$U_{t,r,s} \leq 0; \quad \forall t, r, s \quad (2.15)$$

Chapter 3

Results

This chapter summarizes the findings of the analysis with regard to the research questions. Each section is presented separately to identify the individual moments where the knowledge extracted from each of the disciplines, and their integration is applied.

3.1 Temporal and spatial evolution of El Niño in Peru

This part of our results sections starts by answering the first research question: **Which future El Niño changes can be expected, given the development in the recent past?**

To address this question, we focused first on the El Niño region that is more representative for analyzing this phenomenon and its effects in the country. Based on the studies carried out by researchers from the South American region (e.g. Takahashi et al., 2014), it has been determined that in favor of evaluating the direct impacts of the El Niño phenomenon in countries such as Peru, El Niño 1+2 region should be used. Thus, the specific index (ICEN) based on reconstructed observations serves to identify El Niño events and their intensity.

Evidently, in order to make possible an analysis of past and future states, one has to make use of climate models. In this thesis, we used the outputs of the Max Planck Institute Earth System Model (MPI-ESM-MR). However, the calculated model-based ICEN values cannot be subject to the categories established for the definition of El Niño intensities, since these are supported on ICEN values obtained from observations. Thereby, by using descriptive statistical tools we found that the cumulative density function of the ICEN values obtained using the model and observations datasets are comparable (see figure 3.1). Thus, the low and high quantiles were determined for defining the neutral state set to be from -0.4° to 0.4° for the model-based ICEN values. In the same way, the “strong” category was set to go from 1.0° to 2.0° , and the “extraordinary” greater than 2.0° . Under these categories’ thresholds and during the reference period (1981-2010), we noticed that the model-based ICEN values in contrast with the observations do not include the “extraordinary” category. In fact, the maximum value reached during the reference period is 1.8° . Table 3.1 shows further details of the statistical values and categories defined.

Then, following the definition established for the identification of CEN events in the El Niño 1+2 region that detects a positive event when at least three months of warm conditions are exceeded, strong intensity signals were identified as those months

Table 3.1: Measures of central tendency for the ICEN values using the MPI-ESM-MR & ERSST datasets. El Niño categories' thresholds for both datasets.

	ICEN ERSST	ICEN MPI-ESM
Low Quantile =	-0.70	-0.44
High Quantile =	0.48	0.44
Mean =	0.001	2.58E-05
Max =	4.0	1.8
Neutral	$\langle -1.0; 0.4 \rangle$	$\langle -0.4; 0.4 \rangle$
Weak	$[0.4 ; 0.1 \rangle$	$[0.4 ; 0.7 \rangle$
Moderate	$[0.1 ; 1.7 \rangle$	$[0.7 ; 1.0 \rangle$
Strong	$[1.7 ; 3.0 \rangle$	$[1.0 ; 2.0 \rangle$
Extraordinary	≥ 3.0	≥ 2.0

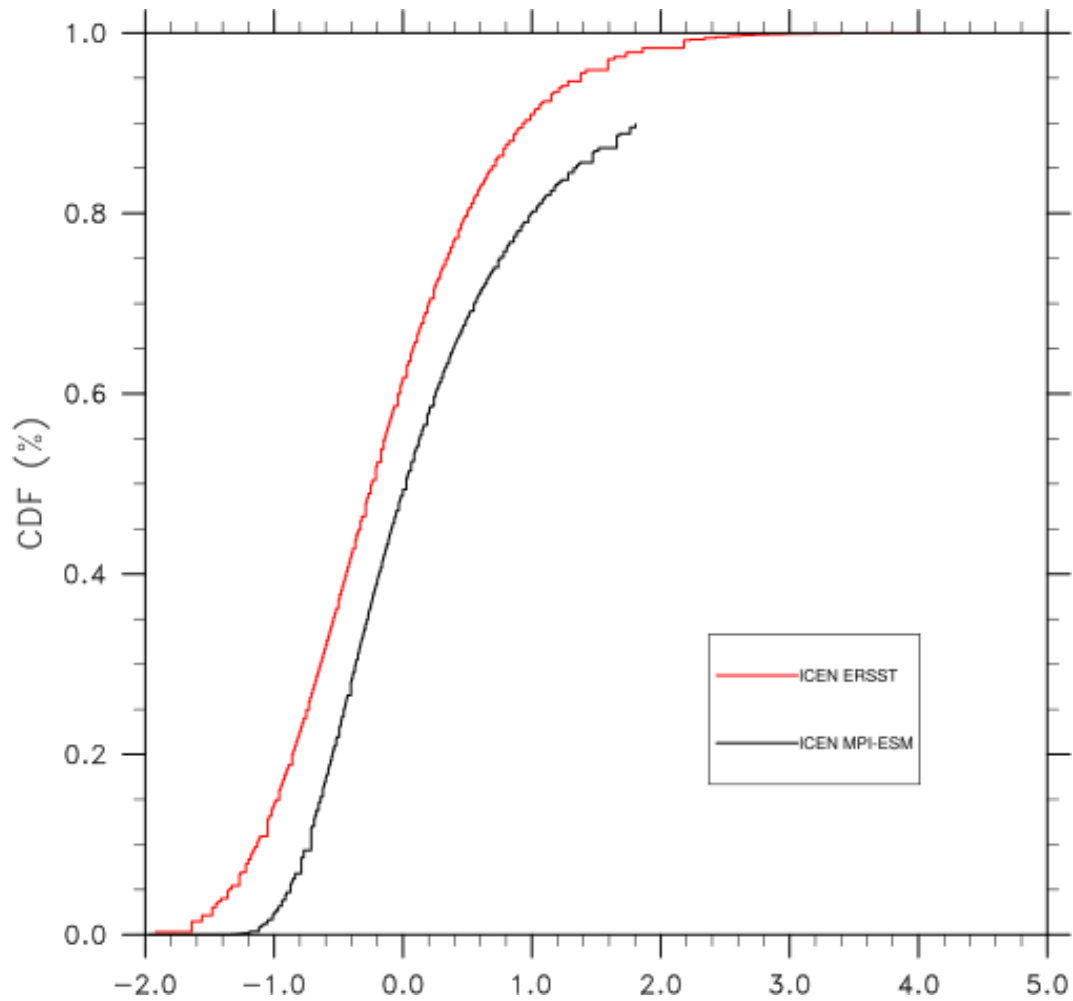


Figure 3.1: Cumulative Density Function of ICEN values obtained with the MPI-ESM-MR and observation datasets

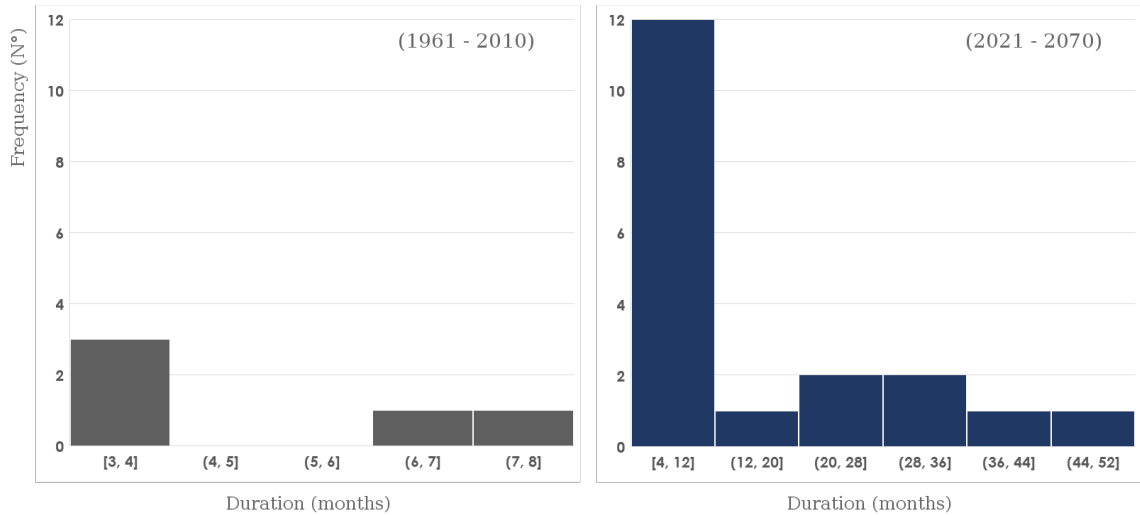


Figure 3.2: Frequency of CEN events for historical simulations 1961-2010 (left) and for the RCP 4.5 scenario 2021-2070 (right).

in which the ICEN showed values greater than 1.7° . Thus, it was possible to notice the important differences in number and duration the CEN events of strong intensity over the past and future (figure 3.2). In general, and answering the second part of the first research question: **Is the suggested increase in number and intensity of future El Niño events and impacts detected?** We found that indeed, there is a clear increase in CEN events over the next 50 years (2021-2070) with respect to the 1961-2010 period. In the latter, the maximum duration of the CEN events is 8 months being the most frequent those lasting from 3 to 4 months, in total 5 events were identified. In contrast, the events identified over the period 2021-2070 have a maximum duration that exceeds 4 years of uninterrupted strong-warm conditions (52 months), the most recurrent last from 4 to 12 months, and in total 19 events were identified (see Appendix B for further details).

The results explained above regarding the increase in the duration of CEN strong events in the future, coincide with the spatial increase of the associated precipitation over the Peruvian territory with respect to the historic period, that can be seen in figure 3.3. In the course of the rainy season in normal conditions, the maximum values of precipitation over the country are recorded in the eastern regions, due to the wet flow coming from the Amazon rainforest that moistens the eastern flank of the Andes cordillera. During CEN events, however, rainfall patterns change significantly over the territory. Lavado and Espinoza (2014) explained the variation of rainfall during El Niño events in Peru, determining that there is a significant rainfall increase in the arid north coastal area. Similar results for the period 1961-2010 were obtained here. The maximum values of precipitation variation were found on the north coast, especially towards the most critical period of the rainy season (Dec-May). As for the 2021-2070 period, the panorama varies significantly, showing extended spatial variations, i.e. not only the north coast is affected by large variations in rainfall but the central and southern coastal areas as well. Towards the first months of the rainy season (SON) the most important variations of precipitation ($\geq 100\%$) are concentrated in the south and central coast and west flank of the Andes. Then, in DJF, variations over 100% are extended from the north to the center of the coastal area and western flank of the Andes. Finally, during MAM, variations over 100% expand equally in the northern and southern coastal zone. These results are important because they

allow detecting temporal and spatial changes that greatly influence the support of adaptation proposals. Firstly, the shift towards a predominantly warm period with a high frequency of strong El Niño events urgently requires actions to mitigate the possible negative effects on ecosystems and social systems. Secondly, the area of affectation where disaster preparedness programs are prioritized is usually identified on the north coast based on past El Niño events. Unlike past events, in the next 50 years El Niño-related impacts are likely to affect the entire coastal strip and the western slope of the Andes. This means that the adaptation plans have to be extended to other territories.

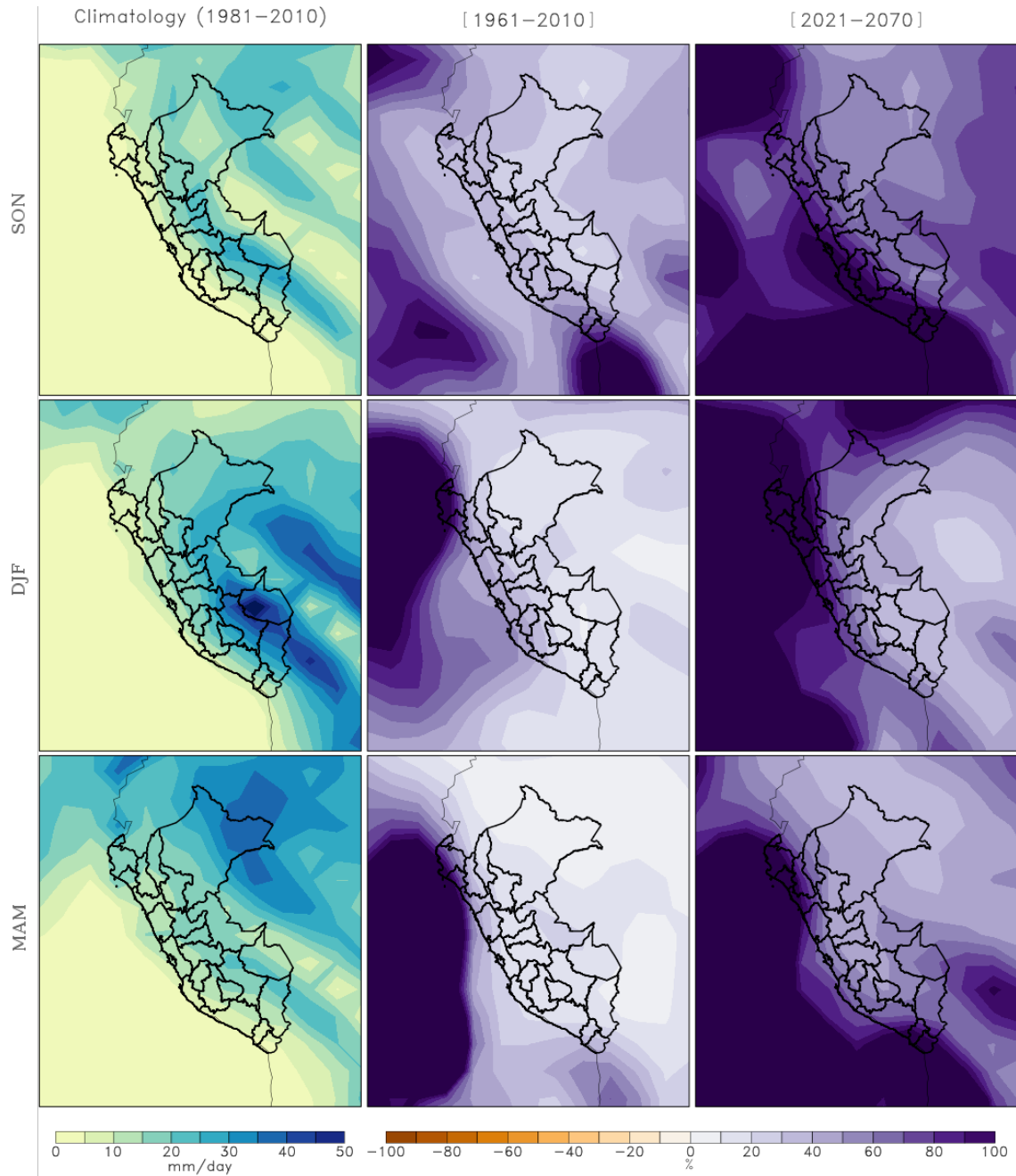


Figure 3.3: Seasonal precipitation during the reference period (1981-2010)(left).Variation of precipitation during CEN events: past events (center) and future events (right).

3.2 Danger Intensity and zones of affectation

The previous findings in regard to the temporal and spatial changes of El Niño in the Peruvian territory bring us to the second research question: **How can that information be included to design an adaptation plan to El Niño impacts?**

From the different precipitation-related impacts during CEN events, stormwater runoff represents a serious threat especially in locations with unstable soil structure. In mountain regions, the excess of stormwater can generate mass movements that ultimately will damage infrastructure, the transport system, agricultural settlements and disruptions to the everyday life (e.g. Moos, 2014).

To determine the affectation areas and estimate the danger to landslides occurrence, we performed a multicriteria analysis that focuses on the analysis of susceptibility to mass movement and the trigger factor referred to as the exceptional precipitation.

The mass movement susceptibility analysis of the Peruvian territory depicted at the provincial level in figure 3.4 shows that the places most susceptible to geodynamic phenomena such as landslides are located in the western zone of the Andes Mountain Range. The highest levels of susceptibility can be found in the central western Andes, while medium and high levels are recorded throughout the mountainous belt from north to south and on both flanks of the Andes. These areas can be easily activated by exceptional rainfall due to their steep slope and soil instability. On the other hand, areas with low susceptibility to mass movement are located in the coastal valleys (far west) and the Amazon region (east) where the slope levels are low.

As for the trigger factor analysis, we incorporated the outputs obtained from the analysis to El Niño of the previous section. That means that the future variation of precipitation during CEN events is taken as a trigger factor to landslides. In figure 3.5, we can see depicted the spatial distribution of the trigger factor at the provincial level, which was obtained according to the intervals of rainfall variation during CEN events for the period 2021-2070. The rain factor map shows rainfall variations ranging from 55 to 600% distributed in five classes. The results show that the landslides trigger factor is intensified in the north and south of the coastal zone and western slopes, predominantly, with rainfall increases greater than 150%. Next in order, we found that along the central western slopes the rain factor takes a level 2 which means that increases of precipitation from 80 to 150% would manifest. While in the Amazonian and Eastern Cordillera regions the intensity of the rain factor is low, meaning that rainfall increases greater than 80% would not be exceeded.

The results of these two analyses are important since the danger associated with landslides during CEN events is highly dependent on the susceptibility and the trigger factor, that influence the stability of sloping areas. Therefore, we derived these factors to a danger matrix from which we obtained a danger intensity map that shows 5 levels of danger. The zones with a very high level of danger are mostly located in the steep areas of the northwest and southwest coast. Most of the mountain chain presents high and intermediate danger levels. Whereas the areas of low danger are located in the dispersed valleys of the far-west coast and the Amazonia (figure 3.6).

Lastly, the multicriteria analysis suggests determining when and with which frequency the event will strike. Thus, it was determined that the probability of future CEN events that strike in the rainy season is 51%, with a recurrence period of 1.9 years.

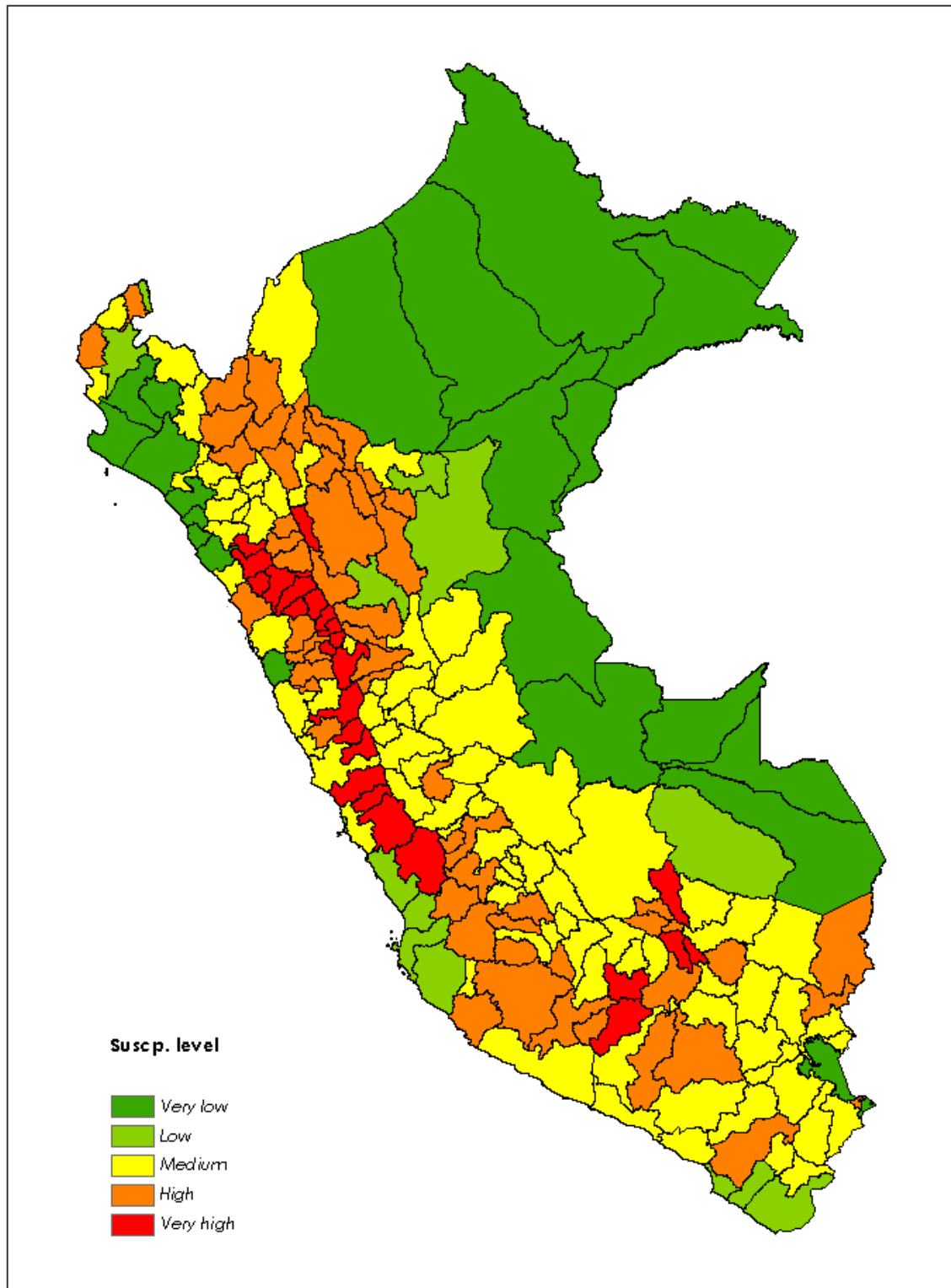


Figure 3.4: Susceptibility to Mass Movement map at a provincial level.

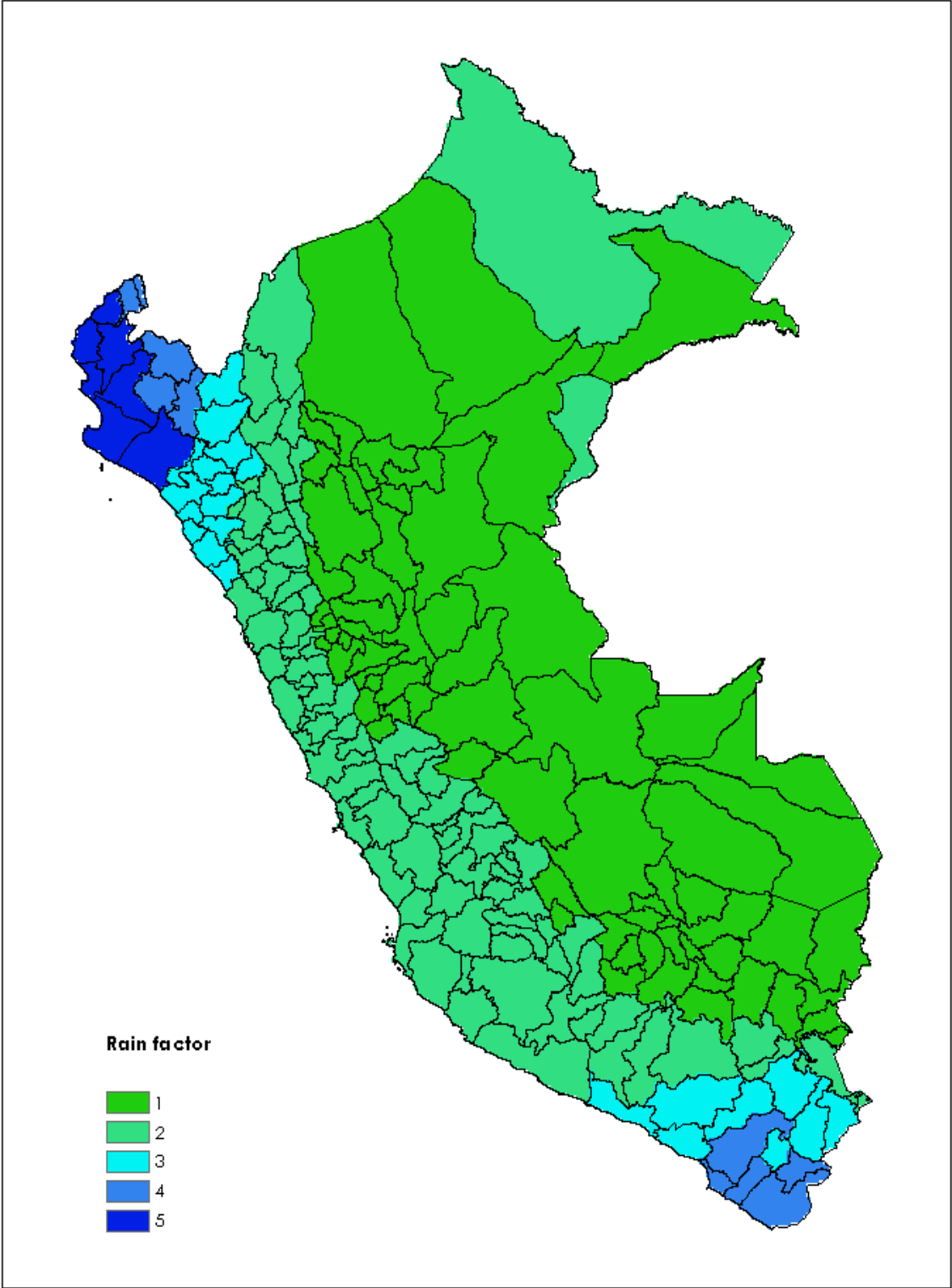


Figure 3.5: Rain factor based on the intervals of variation of precipitation during future (2021-2070) CEN events.

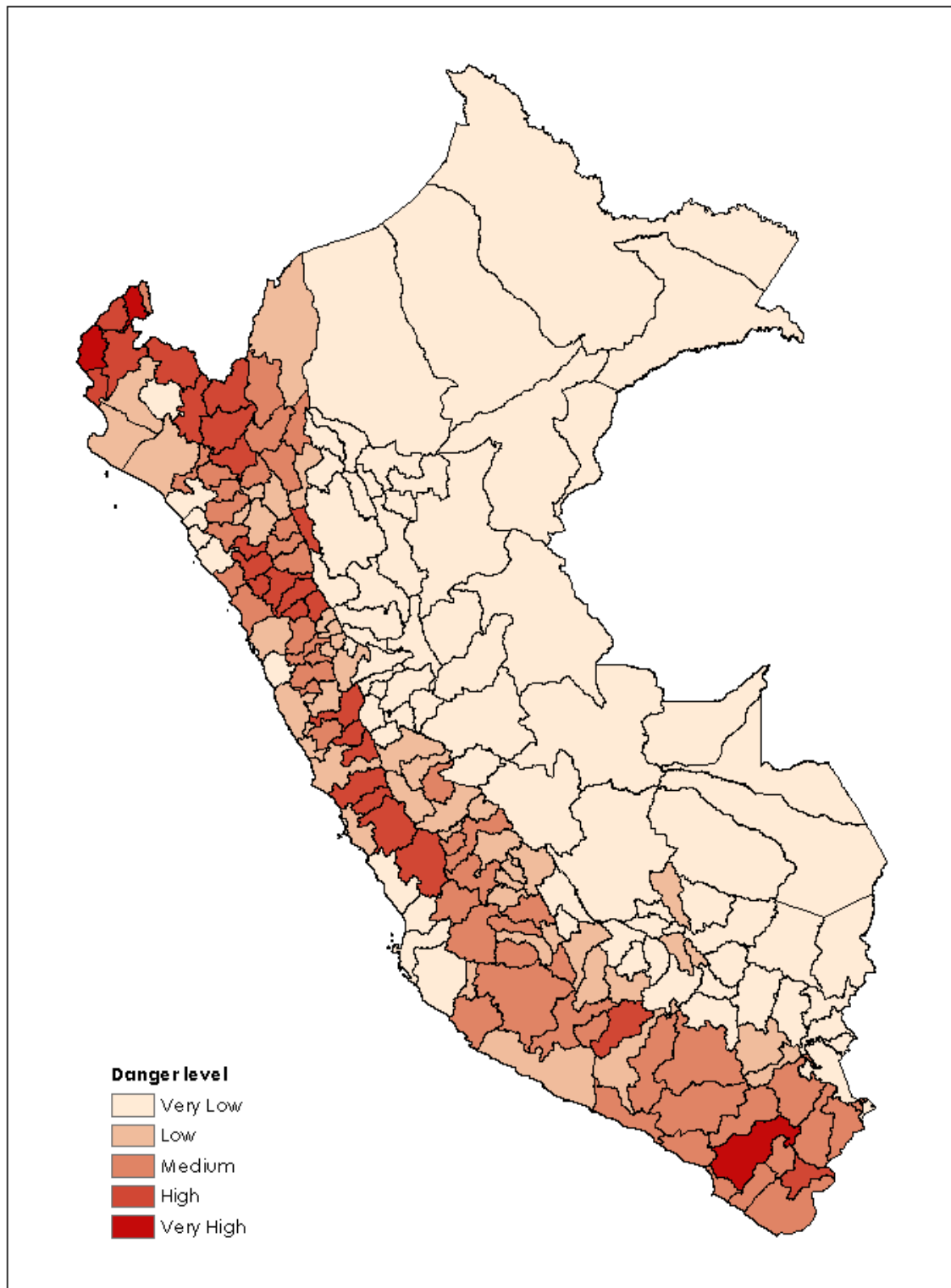


Figure 3.6: Danger intensity map at a provincial level based on the composition of Mass Movement susceptibility and trigger (rain) factor.

3.3 Design of the adaptation strategy

The crucial part of this thesis is the design of the adaptation system, by reason of the third research question: **Which adaptation option for the most recurrent hazard is the most suitable, feasible and cost-effective environmentally, geographically and socioeconomically speaking?** Although the conventional rainwater management systems have reduced the vulnerability to hazards, they cannot cope with the uncalculated effects of future extreme precipitation events (Zölch, 2017). These systems predominantly based on grey infrastructure are designed to handle an exact volume of rainwater, as that represent their design limits. If the magnitude and frequency of extreme rain events increase then the design criteria must change. Therefore, the objective here was to develop an adaptation strategy based on ecosystems. Ecosystems and living organisms create buffers against natural disasters, thereby preventing possible damage. In addition, they constitute a sustainable and economically viable alternative, often more cost effective in the long term than technological investments or the construction and maintenance of infrastructures (Dudley et al., 2015; FEBA, 2017).

Thus, the combination of soil bioengineering approaches and agroforestry systems in sloping regions were taken into account for the design, as those are focused on increasing the stability of the soil in the face of danger. The proposed adaptation design is based on the combination of crops, shrubs, and trees. The percentage of each of these vegetation types varies according to the danger levels and slope values (see table 3.2). The results show that places with high and very high danger levels need of the establishment of arboreal species and shrubs for the stabilization of soils, but not of crops due to the steepness of their slope and the difficult access for the establishment of agricultural systems. As the angle of the slope decreases the allocated percentage of crops can increase, this results in the establishment of agroforestry systems in areas of medium and low danger intensity. In addition, the cropland damage shows that most crop activities affected by landslides are located in high and very high danger zones, with a 5 and 10% of cropland affectation, respectively.

Table 3.2: Danger levels, agricultural damage percentage and allocation of vegetation types.

Danger intensity	Danger	%Ha Damage	% Trees	% Shrubs	% Crops
Very Low	1	0	17	9	74
Low	2	1	27	18	55
Medium	3	2	32	21	47
High	4	5	45	55	0
Very High	5	10	44	56	0

We also calculated the reduction of danger when implementing the ecosystem-based adaptation criterion in all affected lands. Analyzing the equation (2.3) for the calculation of susceptibility, we found that it would be possible to reduce the contribution of susceptibility for vegetation cover and hydrogeology in the total calculation of the susceptibility to mass movement by 15%.

For the purposes of this thesis, the economic impact of the implementation of this design on croplands was evaluated by optimizing the country's surplus on agriculture when the adaptation strategy takes place. Our model shows that opting for adaptation without negatively affecting the total welfare will require to obtain a Side Benefit

LEVEL 2 as a minimum requirement for the implementation of protective stripes. In fact, figure 3.7 shows that land for crop adaptation is suggested to increase as side benefit increases. Side benefit increases by 50 USD/ha in each level, that means that the maximum side benefit considered here is 300 USD/ha , which is less than the estimates that consider that ecosystem services due to agroforestry can go up to 400 USD/ha (The Economics of Ecosystems and Biodiversity (TEEB), 2014). Consequently, when comparing the total welfare of different side benefits' scenarios, we found an increase in welfare as the side benefits increases (see figure 3.8). Side benefit LEVEL 1 means no adaptation takes place, and as such welfare under that condition is lower than when adaptation is applied.

Another outcome is the map of the distribution of adaptation sites when the maximum side benefits are considered (figure 3.9). Those places are mostly located on both sides of the Andes Cordillera, and on the north coast, places commonly used for agriculture activities which also happen to be located in landslides danger areas. The coloration indicates the number of hectares allocated for adaptation in each homogeneous unit. The intensity of cropland adaptation in the north coast and Andes slopes gives an indication of the potential of the adaptation design at decreasing the overall danger levels and possible damages in agricultural systems.

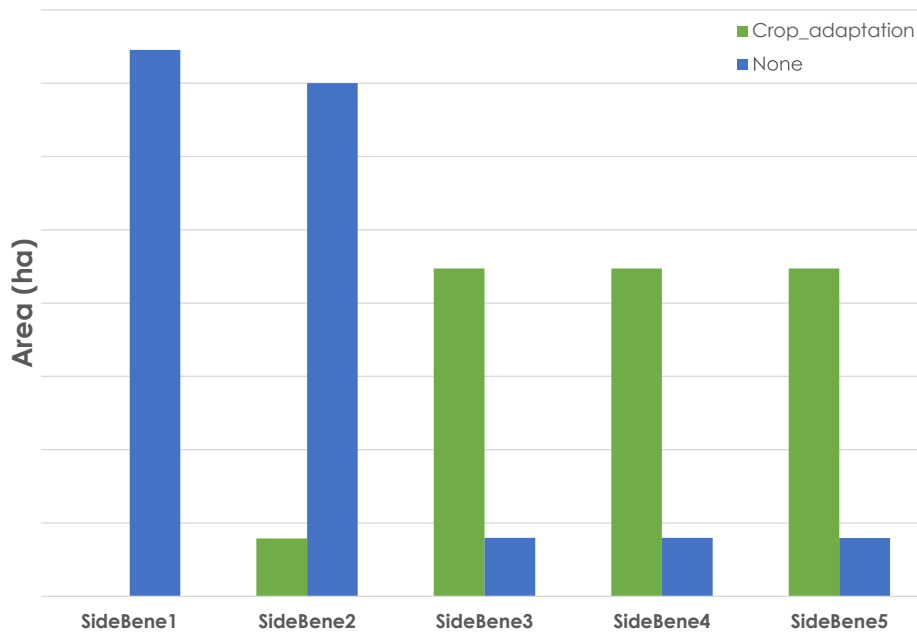


Figure 3.7: Effect of the side benefits in the cropland allocation for adaptation.

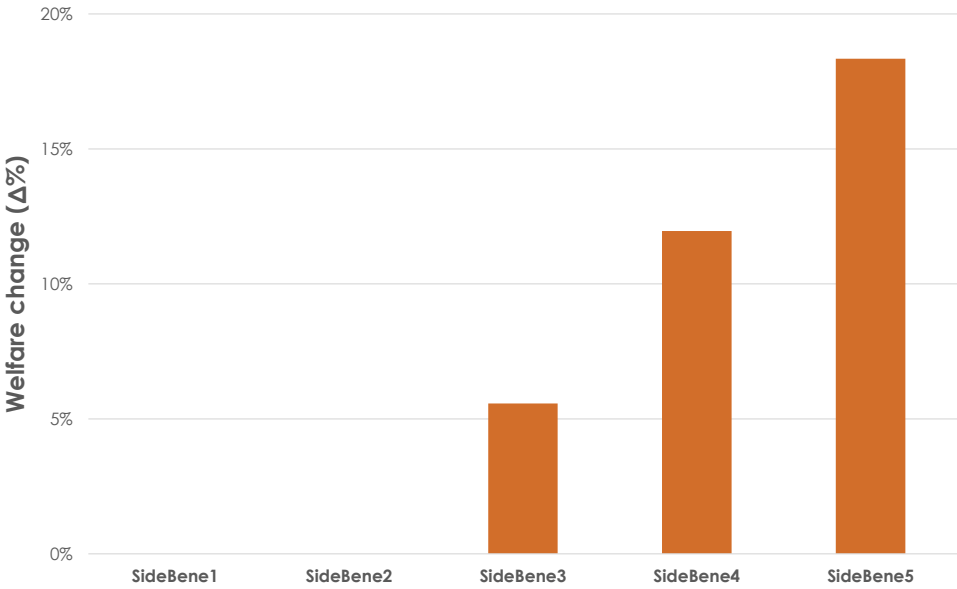


Figure 3.8: Effect of adaptation side benefits in the total welfare compared with the no adaptation condition.

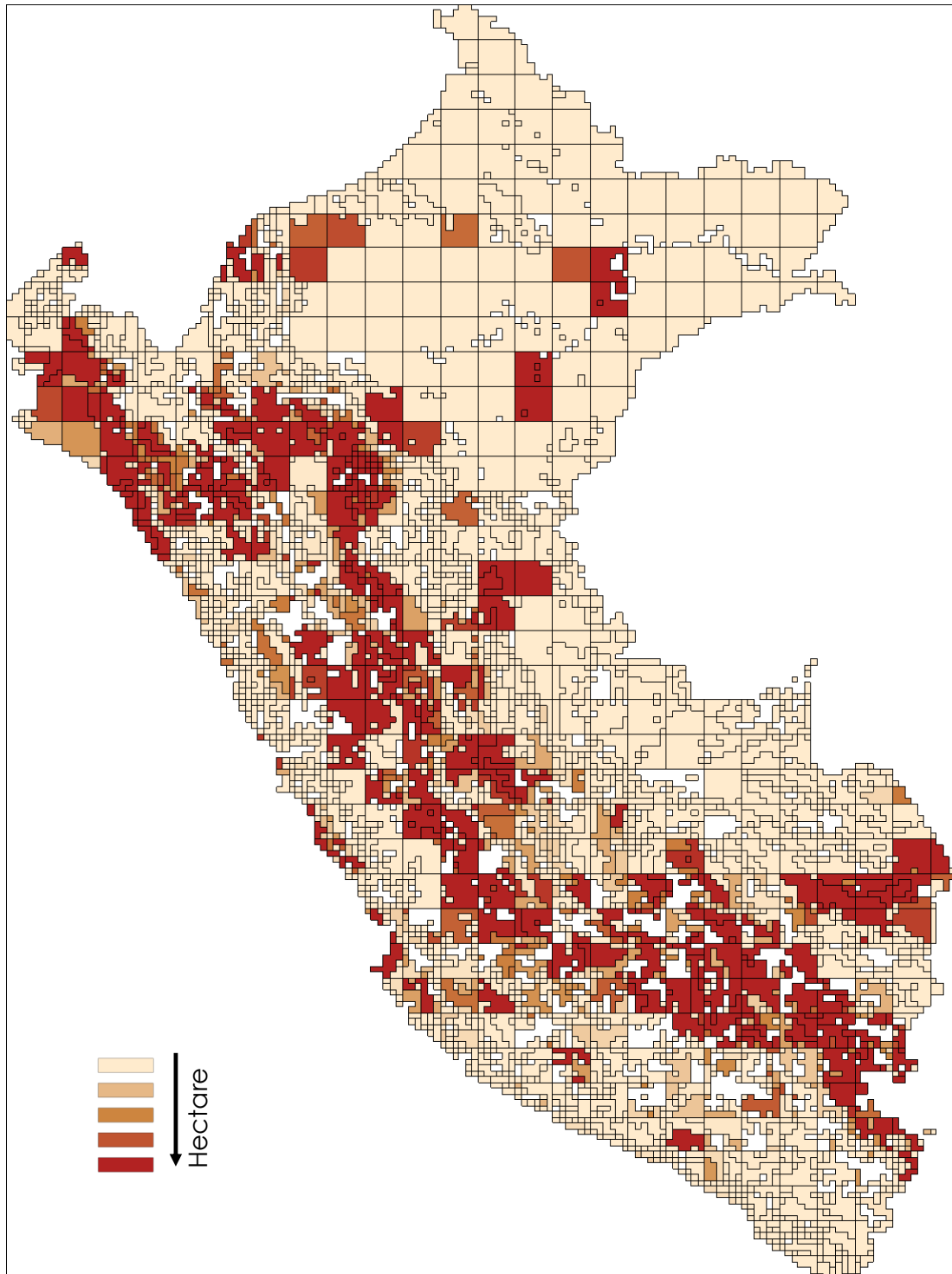


Figure 3.9: Map of cropland adaptation sites with a maximum Side Benefit.

Chapter 4

Discussions

This thesis proposes a novel, interdisciplinary, scientific and engineering-based adaptation approach to take advantage of and cope with the impacts of heavy precipitations in Peru during Coastal-El Niño events. The novelty is the result of the integration of: a) climate projections and geophysical analyses; as support for b) the identification of zones in danger to mass movements due to the combined effects of heavy precipitations and unstable terrains; that will serve as conditioning for, c) the design of the adaptation strategy based on ecosystems; and the consequent, d) inclusion of an agroeconomic optimization and feasibility evaluation.

The approach consisted of climatic modelling (using the outputs of MPI-ESM-MR), danger analysis, ecosystem-based engineering design and agroeconomic modelling (with ENAAM). Although it proved to be well-suited to the purpose of this thesis, some methodological limitations are to be considered and discussed in the following sections.

4.1 Advantages and limitations of the climate analysis

Normally, the risk scenarios of the impacts of El Niño are based on past events detected using the central Pacific El Niño indexes. The present thesis, unlike other studies, took into consideration the region El Niño 1+2, i.e. coastal-El Niño, as a focus area for the analysis of past and future El Niño states impacts in Peru following the recommendations of the ENFEN.

Additionally, we based our study on the analysis of climate projections obtained from the MPI-ESM-MR, whose outputs have already been tested for Peru. SENAMHI (2014) highlighted the ability of the MPI model at representing well the orographic conditions and therefore the precipitation patterns in the country. Same results were found in this study reinforcing our results for El Niño projections. The climatology of precipitation represented spatially by the model corresponds to the actual observed precipitation distribution during the rainy season. However, spatial resolution plays a role in representing local conditions, that due to the restricted ability of the employed model -approximate resolution 200km- is not possible to observe. Some studies (e.g. SENAMHI, 2014) suggest that for a better simulation of the local variations will be necessary to perform downscaling operations that were not considered here.

Regarding future El Niño states, we found in agreement with other studies (e.g. Cane, 2005; Ove Hoegh-Guldberg et al., 2018), that the frequency, number, and du-

ration of future episodes are suggested to increase. That supports the argument that the risk or danger scenarios should be built taking climate projections as input and, thereby, dismissing the assumptions of building impact scenarios based on past events. Our results show that future affectation areas are likely to expand, besides the north that used to be primarily affected in past events, towards the central and south coast, as well as the western slope of the Andes Cordillera. These results are backed up in the last El Niño in 2016-17 which showed damages in the southern and central areas of Peru as well.

It should be taken into consideration that this study focuses on the rainy season, because of the intensification of the precipitation impacts in warm conditions, in addition to the great socio-economic importance of the production activities within this season. Nevertheless, one should possibly consider future changes in the patterns of precipitation that would disrupt the dry and wet states.

4.2 Limitations of the danger analysis

Ideally, this kind of studies should consider risk scenarios. Our study, however, has to be read as a danger scenario analysis. Since the evaluation of risk entails a vulnerability analysis that is beyond the scope of this paper. Therefore, we built our study on the analysis of the susceptibility obtained from Villacorta et al. (2015) plus the climate analysis described previously. Both pieces of information come with different spatial resolutions that in the end, can constitute a problem. For our purposes, we expressed all our results at a provincial level which also creates uncertainties when taking homogeneous conditions, that differ from reality, for entire provinces.

4.3 Advantages and limitations of the adaptation design

With respect to the adaptation plans, currently, preparation programs are implemented especially in vulnerable areas. However, in its design and application, shortcomings are observed that cause a dynamic that fails to take the opportunity to foster adaptive strategies linked to the trajectories of overcoming vulnerability (Canales et al., 2014). These measures only seek to avoid the potential damages associated with the occurrence of extreme events, but do not attempt to adapt the environments to the new climatic conditions, and thereby take advantage of the effects associated with them.

Hence, in this thesis, we consider a multifunctional adaptation approach based on ecosystem services, as part of an overall adaptation strategy to landslides danger while it gives other socio and economic co-benefits for local communities. The International Seminar "Dry Forest and Desertification" recognizes that the dry forest is reduced between 7,000 and 14,800 ha per year (FAO (Food and Agricultural Organization of the United Nations), 2018). This forest can only be compensated by natural processes such as the "El Niño" phenomenon, demonstrating the positive effects of precipitation increases in ecosystems.

To our knowledge, there are no guidelines that include the technical aspects of adaptation options for each type of hazard. Moreover, adaptation is highly dependant on the contextual scenario, which means that some experiences cannot be transferred, as they are, to other areas. Fortunately, there are some experimental studies on soil

stabilization in sloping areas of the Alps and Himalayas which provide empirical input for our design. Thus, rough estimates and standard values taken from the literature were chosen to represent, for example, the type of vegetation needed, the proportion of vegetation cover, or the minimum spacing between vegetation species. However, it is possible that the chosen values are not well represented, and therefore, not applicable to specific contexts since the design is a combination of techniques and assumptions. In the same manner, it is still unknown how much land is lost even after applying the proposed adaptation option. Empirical measurements of those variables in the study area would clarify this issue.

4.4 Limitation of the optimization model

Simulating the entire socioeconomic effect of the proposed adaptation design is beyond the scope of this study since it would require disproportionate effort to analyze each economic sector. Therefore, here we tested the agro-economic feasibility of the adaptation design, relying on a mathematical experimental setup only. The agro-economic model for optimization also shows some limitations, starting from the data availability. For the calibration of the model, we used data from the FAO database at a country level, rough estimates of crop production at a provincial level for one year only, and 12 crops species which were not selected carefully, i.e. they are not necessarily representative for the country. Then, the agricultural land damaged for each danger level was estimated based on the last El Niño episode. However, as it was argued before, the affectation areas in the future may change, and therefore, those estimates may be wrong.

On the other hand, to fully evaluate the agro-economic benefits obtained from adaptation, more information about the costs and benefits of vegetation species needs to be included as they are vital for the decision towards adaptation. For instance, it is likely that other ecosystem services are provided when ecosystem-based adaptation measures are implemented to mitigate heavy rain events, such as the support of vegetation in climate change mitigation by sequestering and storing carbon emissions, enhancing the water cycle, filtering air pollutants, and increasing biodiversity (e.g. Zölch, 2017).

Returning to the broader perspective about the specificity of the adaptation design to the context, we need to keep in mind that the proposed strategy cannot directly be applied on the ground, but needs of a further analysis of the area in which it will operate. Nonetheless, this study can serve as an estimation of the potential for landslide mitigation offered by the implementation of vegetation. The strategy shows that EbA is a valuable way to counteract projected impacts and reduce the susceptibility of the sloping areas to heavy rains.

Chapter 5

Conclusions

Based on our analysis of climate and geophysical information for the design and evaluation of an adaptation strategy to heavy precipitation impacts during future coastal-El Niño events, we conclude:

- Future strong coastal-El Niño events are suggested to increase in the next 50 years (2021-2070) compared to the 1961-2010 period, with a 51% probability of occurrence in the rainy season and a return period of 1.9 years.
- During CEN events, variations of precipitation greater than 100% are suggested to equally affect the northern and southern coast of Peru, as well as, part of the sloping areas of the western side of the Andes Cordillera.
- In Andean valleys and mountain regions, stormwater runoff and the consequent mass movement due to unstable soil conditions are the major precipitation-related impacts during CEN events, causing up to 10% agricultural damages.
- The danger intensity - which is defined as a function of the mass movement susceptibility levels and the trigger factor - can be used to estimate the adaptation design parameters by exploring engineering techniques for stabilizing sloping areas.
- The employed soil bioengineering techniques together with the Slope Agroforestry system result in a proposed adaptation strategy that includes a combination of different proportions of trees, shrubs, and crops according to the danger intensities, which in turn might reduce susceptibility levels by roughly 15%.
- The agro-economic model shows that in the presence of an El Niño event of strong intensity, adaptation is possible when side benefits are high enough to maintain welfare.
- Compared to the no adaptation condition, there is a welfare change that goes roughly up to 18% when applying the adaptation strategy.

Ecosystems provide a way to counteract the impacts of climate hazards while providing socio-economic benefits. Despite obvious limitations, the findings support that interdisciplinary research efforts can support the understanding of impacts and opportunities of climate hazards, and improve the transfer of knowledge from science to practice for successful adaptation strategies by using the benefits of ecosystems.

5.1 Outlook

Future research should include empirical data in order to get more practical results which are useful for practitioners in natural hazard management. For instance, the limitations presented in the discussion chapter should be addressed. Ultimately, the results of the adaptation design should be connected to actual field work. A pilot project could be implemented in one specific area of affectation, aiming at collecting more data for the improvement of the design and agroeconomic model.

Bibliography

- Arkema, K. K., R. Griffin, S. Maldonado, J. Silver, J. Suckale, and A. D. Guerry
2017. Linking social, ecological, and physical science to advance natural and nature-based protection for coastal communities. *ANNALS OF THE NEW YORK ACADEMY OF SCIENCES*, 1399(1, SI):5–26.
- Bischetti, G. B., E. A. Chiaradia, V. D’Agostino, and T. Simonato
2010. Quantifying the effect of brush layering on slope stability. *Ecological Engineering*, 36(3):258–264.
- Bobrowski, J.
1997. Soil Bioengineering with Woody Vegetation for Slope Stabilization. *Student On-Line*, 2(7):1–4.
- Canales, L., M. Gallardo, and L. Angulo
2014. Climate Change in the Andes: agreements and disagreements between science and local knowledge. Technical report, Programa de Adaptación al Cambio Climático, Lima, Perú.
- Cane, M. A.
2005. The evolution of El Niño, past and future. *Earth and Planetary Science Letters*, 230(3-4):227–240.
- CENEPRED
2012. Escenarios de Riesgos ante la Probabilidad de currencia del Fenómeno El Niño. Technical report, Ministerio del Ambiente del Perú, Lima, Perú.
- Damonte, G., M. Glave, and R. B. D. Mendoza
2018. *Recursos naturales, industrias extractivas y conflictos sociales*. Lima, Perú: [publisher unknown].
- Dudley, N., C. Buyck, N. Furuta, C. Pedrot, F. Renaud, and K. Sudmeier-Rieux
2015. *Protected Areas as Tools for Disaster Risk Reduction. A handbook for practitioners*, volume 134.
- ENFEN
2012. Definición operacional de los eventos El Niño y La Niña y sus magnitudes en la Costa del Perú. Technical report.
- FAO (Food and Agricultural Organization of the United Nations)
2018. FAOSTAT Database.
- FEBA
2017. Making Ecosystem-based Adaptation Effective: A Framework for Defining

- Qualification Criteria and Quality Standards. Technical Report May 2017, Friends of Ecosystem-based Adaptation.
- French, A. and R. Mechler
2017. Managing El Nino Risks under Uncertainty in Peru: Learning from the past for a more disaster-resilient future. Technical Report September.
- Galarza, E., J. Kámiche, M. Collado, and A. Pacheco
2012. Impactos del Fenómeno El Niño (FEN) en la economía regional de Piura , Lambayeque y La Libertad. Technical report, Lima, Perú.
- Galvez, J.
2017. A sequence of the apparent development of the 2016-17 “Coastal” El Nino event and associated rainfall.
- Gassman, P., J. Williams, V. Benson, R. C. Izaurralde, L. M. Hauck, C. A. Jones, J. D. Atwood, J. R. Kiniry, and J. D. Flowers
2005. Historical development and applications of the EPIC and APEX models. *Director*, P. 45.
- Giorgetta, M. A., J. Jungclaus, C. H. Reick, S. Legutke, J. Bader, M. Böttinger, V. Brovkin, T. Crueger, M. Esch, K. Fieg, K. Glushak, V. Gayler, H. Haak, H.-D. Hollweg, T. Ilyina, S. Kinne, L. Kornblueh, D. Matei, T. Mauritsen, U. Mikolajewicz, W. Mueller, D. Notz, F. Pithan, T. Raddatz, S. Rast, R. Redler, E. Roeckner, H. Schmidt, R. Schnur, J. Segschneider, K. D. Six, M. Stockhause, C. Timmreck, J. Wegner, H. Widmann, K.-H. Wieners, M. Claussen, J. Marotzke, and B. Stevens
2013. Climate and carbon cycle changes from 1850 to 2100 in MPI-ESM simulations for the Coupled Model Intercomparison Project phase 5. *Journal of Advances in Modeling Earth Systems*, 5(3):572–597.
- Grizzetti, B., C. Liqueste, P. Antunes, L. Carvalho, N. Geamănă, R. Giucă, M. Leone, S. McConnell, E. Preda, R. Santos, F. Turkelboom, A. Vădineanu, and H. Woods
2016. Ecosystem services for water policy: Insights across Europe. *Environmental Science and Policy*, 66:179–190.
- INDECI
2016. Probable Escenario de Riesgo ante la Ocurrencia del Fenómeno El Niño Extraordinario y lluvias intensas 2015 - 2016. Technical report, Ministerio del Ambiente del Perú, Lima, Perú.
- INDECI
2017. Boletín Estadístico Virtual de la Gestión Reactiva. Technical report.
- INDECI, World Food Programme, Save the Children, and USAID
2017. *Fortaleciendo la respuesta ante desastres en el Perú*.
- Johnson, C. A. and K. Krishnamurthy
2010. Dealing with displacement: can “social protection” facilitate long-term adaptation to climate change? *Global Environmental Change*, 20:648–655.
- Lagos, P., Y. Silva, E. Nickl, and K. Mosquera
2008. El Niño - Related precipitation variability in Perú. *Advances in Geosciences*, 14(July 2014):231–237.

- Lampadia
2015. La agricultura peruana tiene un gran futuro.
- Lavado, W. and J. Espinoza
2014. Impactos de El Niño y La Niña en las lluvias del Perú (1965-2007). *Revista Brasileira de Meteorologia*, 29(2):171–182.
- Lenton, T. M., H. Held, E. Kriegler, J. W. Hall, W. Lucht, S. Rahmstorf, and H. J. Schellnhuber
2009. Tipping elements in the Earth System. *Proceedings of the National Academy of Sciences*, 106(49):20561–20563.
- Martínez, A. and K. Takahashi
2017. ¿El Niño Costero o Fenómeno El Niño?
- Martinez-Alonso, C., B. Locatelli, R. Vignola, and P. Imbach
2010. *Adaptación al cambio climático y servicios ecosistémicos en América Latina. Libro de actas del Seminario Internacional sobre Adaptación al Cambio*, number 506. Catie.
- Ministerio del Medio Ambiente del Perú
2015. Mapa de susceptibilidad física del Perú.
- Ministerio del Medio Ambiente del Perú
2016. *El Perú y el Cambio Climático Tercera Comunicación*.
- Moos, C.
2014. *How does forest structure affect landslide susceptibility?* PhD thesis, ETH Zürich.
- Niño-Zarazúa, M., A. Barrientos, S. Hickey, and D. Hulme
2012. Social Protection in Sub-Saharan Africa: Getting the Politics Right. *World Development Elsevier Science*, 40(1):163–176.
- Ove Hoegh-Guldberg, D. Jacob, M. Taylor, and E. al
2018. Impacts of 1.5°C global warming on natural and human systems. *Global Warming of 1.5 C - IPCC's special assessment report*.
- PNUD Cuba
2014. *Metodología para la determinación de Riesgos de Desastres a Nivel Territorial*.
- Raut, R. and O. T. Gudmestad
2017. Use of bioengineering techniques to prevent landslides in Nepal for hydropower development. *International Journal of Design and Nature and Ecodynamics*, 12(4):418–427.
- Roshetko JM, Mercado Jr AR, Martini E, P. D.
2017. Agroforestry in the uplands of Southeast Asia.
- Sabates-Wheeler, R. and S. Devereux
2010. Cash transfers and high food prices: Explaining outcomes on Ethiopia's Productive Safety Net Programme.

SENAMHI

2009. Climate Scenarios for Peru to 2030. Technical report, Ministerio del Ambiente de Perú, Lima, Perú.

SENAMHI

2014. Statistical downscaling of climate change scenarios. Technical Report November, Ministerio del Ambiente del Perú, Lima, Perú.

Shrestha, A., E. GC, R. Adhikary, and S. Rai

2012. *Resource Manual on Flash Flood Risk Management: Module-2. Non-Structural Measures*. Kathmandu, Nepal: International Centre for Integrated Mountain Development.

Takahashi, K., K. Mosquera, and J. Reupo

2014. El Índice Costero El Niño (ICEN): historia y actualización.

Tej, P. and R. Harold

1994. Sloping Agricultural Land Technology (SALT).

The Economics of Ecosystems and Biodiversity (TEEB)

2014. TEEB Valuation Database.

US Department of Agriculture Natural resource Conservation service

1992. Soil Bioengineering for Upland Slope Protection. In *Engineering Field handbook*, chapter Chapter 18, P. 61. Washington, USA: [publisher unknown].

Villacorta, S., L. Fidel, and B. Zavala Carrion

2015. Mapa de amenazas por movimientos en masa. *Revista de la Asociación Geológica Argentina*, 69(3):1.

Zölch, T. M.

2017. *The potential of ecosystem-based adaptation: Integration into urban planning and effectiveness for heat and flood mitigation*. PhD thesis, Technische Universität München.

Appendices

Appendix A: Allocation of vegetation types

Here, we show the resource allocation on the field based on the parameters of the adaptation design employing the following variables: horizontal distance-A (HD_A) and horizontal distance-B (HD_B).

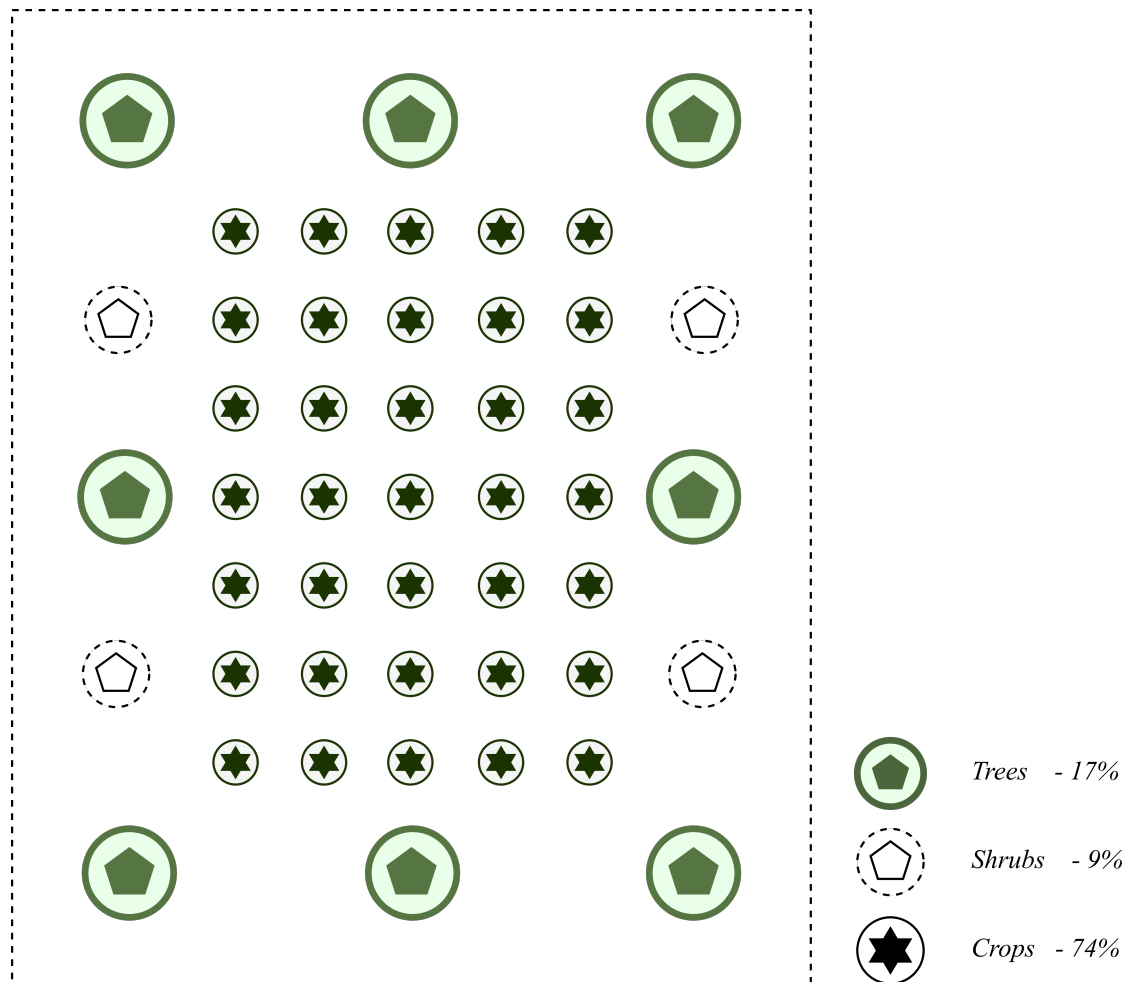


Figure A.1: Resource allocation for "VERY LOW" danger level.

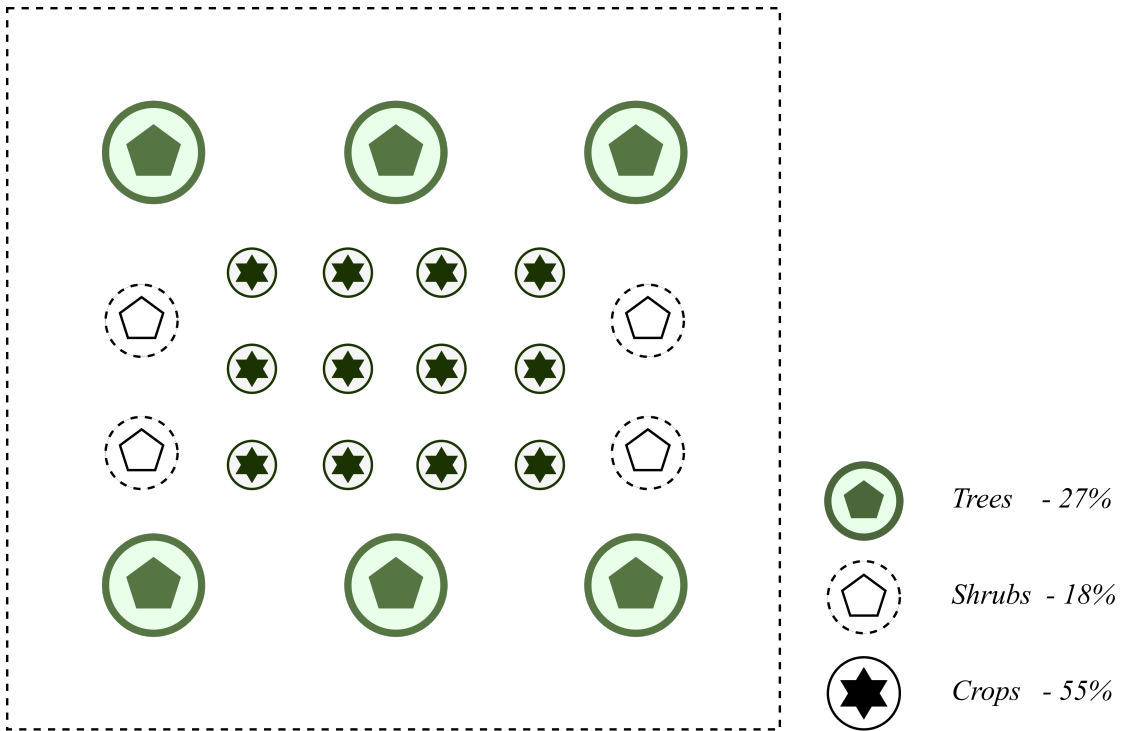


Figure A.2: Resource allocation for "LOW" danger level.

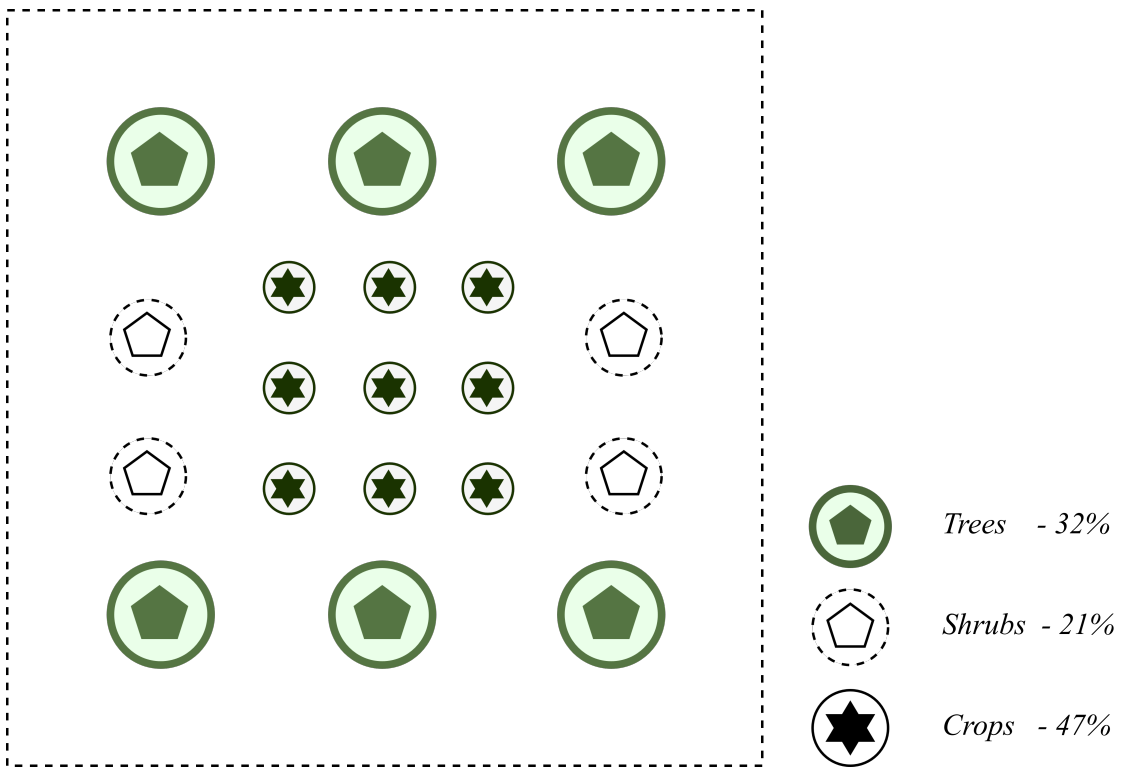


Figure A.3: Resource allocation for "MEDIUM" danger level.

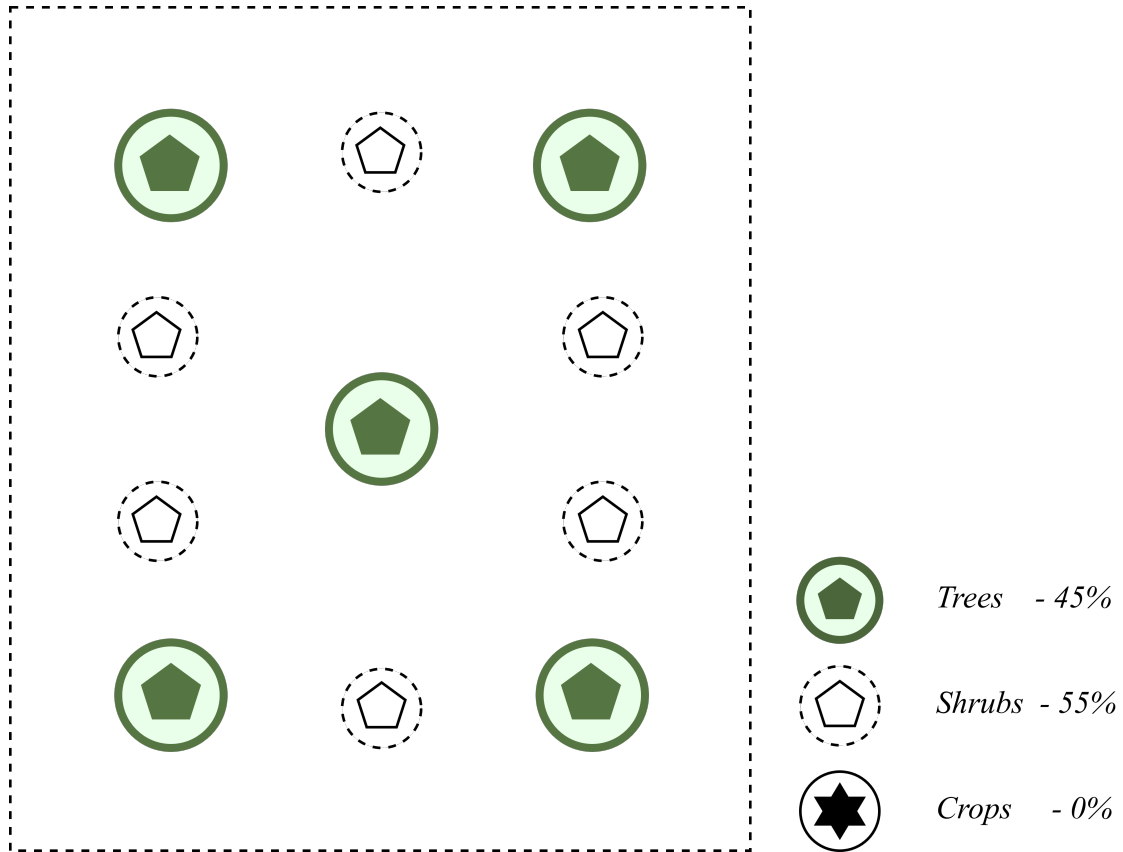


Figure A.4: Resource allocation for "HIGH" danger level.

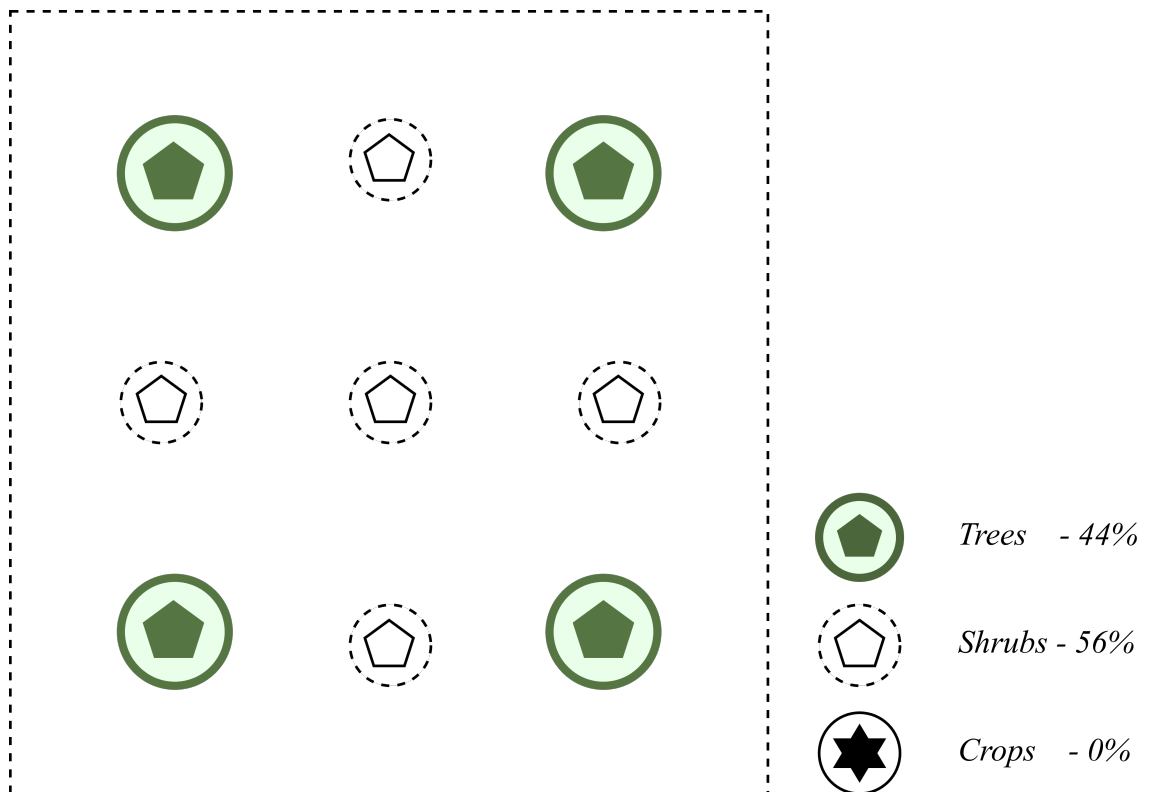


Figure A.5: Resource allocation for "VERY HIGH" danger level.

Appendix B: Coastal-El Niño events

Table B.1: CEN events identified during the periods 1961-2010 and 2021-2070.

a)						
	Initial year	Initial month	Final year	Final month	Duration (months)	Magnitude
1961-2010	1996	June	1996	December	7	Strong
	1997	April	1997	June	3	Strong
	1999	June	2000	January	8	Strong
	2004	December	2005	February	3	Strong
	2010	September	2010	December	4	Strong
b)						
2021-2070	2025	April	2025	August	4	Strong
	2026	April	2027	February	11	Strong
	2018	November	2029	March	5	Strong
	2030	October	2031	January	4	Strong
	2031	November	2032	August	10	Strong
	2033	June	2033	September	4	Strong
	2036	May	2037	March	11	Strong
	2040	January	2041	June	18	Strong
	2042	December	2043	April	5	Strong
	2044	December	2045	June	7	Strong
	2046	April	2046	October	7	Strong
	2048	January	2050	May	29	Strong
	2050	September	2053	April	32	Strong
	2054	June	2056	April	23	Strong
	2057	November	2058	April	6	Strong
	2058	December	2059	May	6	Strong
	2060	March	2063	October	44	Strong
2064	March	2068	April	50	Strong	
2069	February	2070	October	21	Strong	

Table B.2: El Niño signal within the sub-seasons of the Rainy season.

a)					
	Initial year	Final year	SON	DJF	MAM
1961-2010	1996	1996	1996		
	1997	1997			1997
	1999	2000	1999	2000	
	2004	2005		2005	
	2010	2010	2010		
b)					
2021-2070	2025	2025			2025
	2026	2027	2026	2027	2026
	2018	2029		2029	
	2030	2031	2030	2031	
	2031	2032		2032	2032
	2033	2033			
	2036	2037	2036	2037	
	2040	2041	2040	2040-2041	2041
	2042	2043		2043	2043
	2044	2045		2045	2045
	2046	2046	2046		2046
	2048	2050	2048-2049	2048-2049- 2050	2048-2049- 2050
	2050	2053	2050-2051- 2052	2051-2052- 2053	2051-2052- 2053
	2054	2056	2054-2055	2055-2056	2055-2056
	2057	2058		2058	2058
	2058	2059		2059	2059
	2060	2063	2060-2061- 2062-2063	2061-2062- 2063	2060-2061- 2062-2063
	2064	2068	2064-2065- 2066-2067	2065-2066- 2067-2068	2064-2065- 2066-2067- 2068
	2069	2070	2069-2070	2070	2069-2070

Appendix C: Cropland distribution vs. danger levels

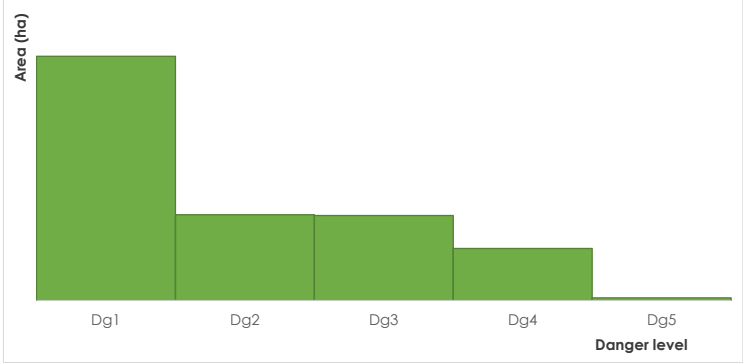


Figure A.6: Normal cropland distribution according to the danger levels.

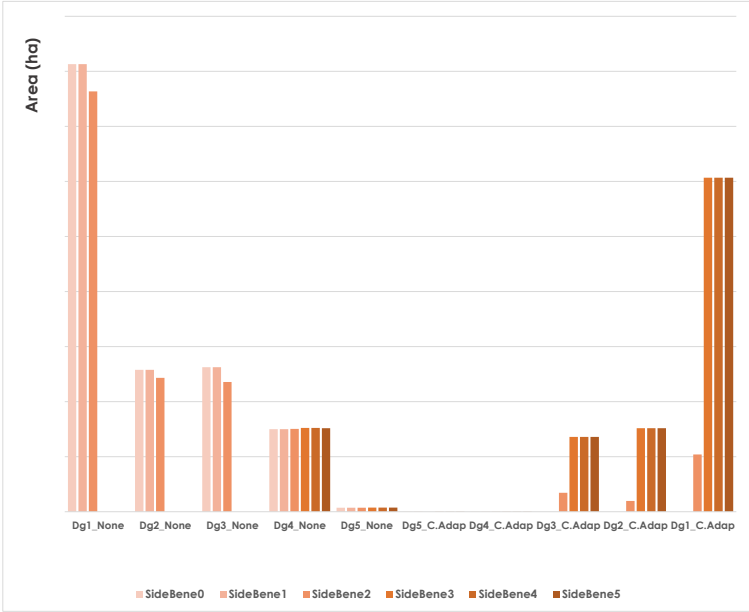


Figure A.7: Cropland distribution according to the danger levels and side benefits of adaptation.

Appendix D: Cropland adaptation according to the Side Benefits

Here we show the levels of adaptation when side benefits increase.

- Side benefit 1: 100 USD/ha
- Side benefit 2: 150 USD/ha
- Side benefit 3: 200 USD/ha

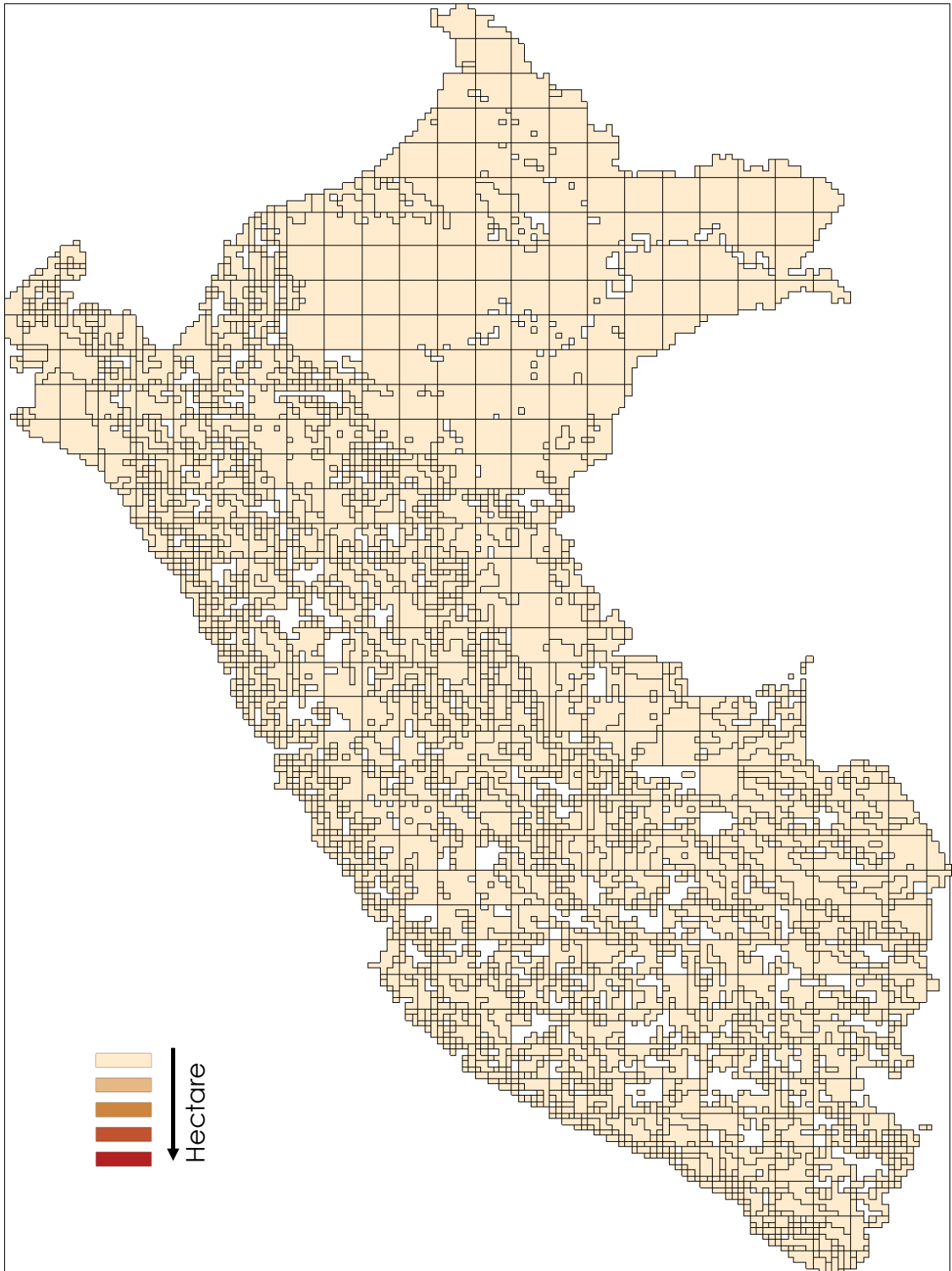


Figure A.8: Cropland adaptation with Side benefit LEVEL 1.

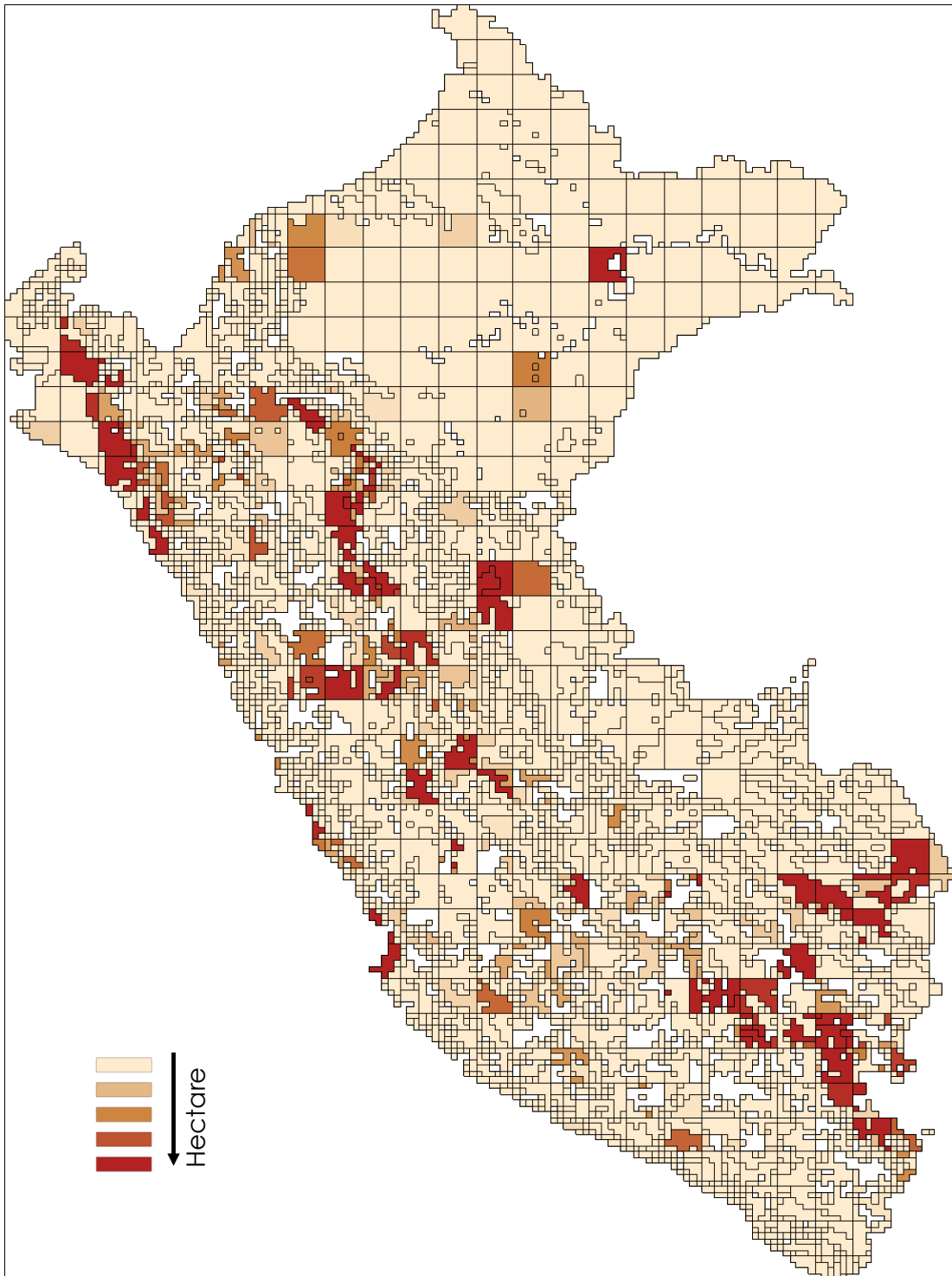


Figure A.9: Cropland adaptation with Side benefit LEVEL 2.

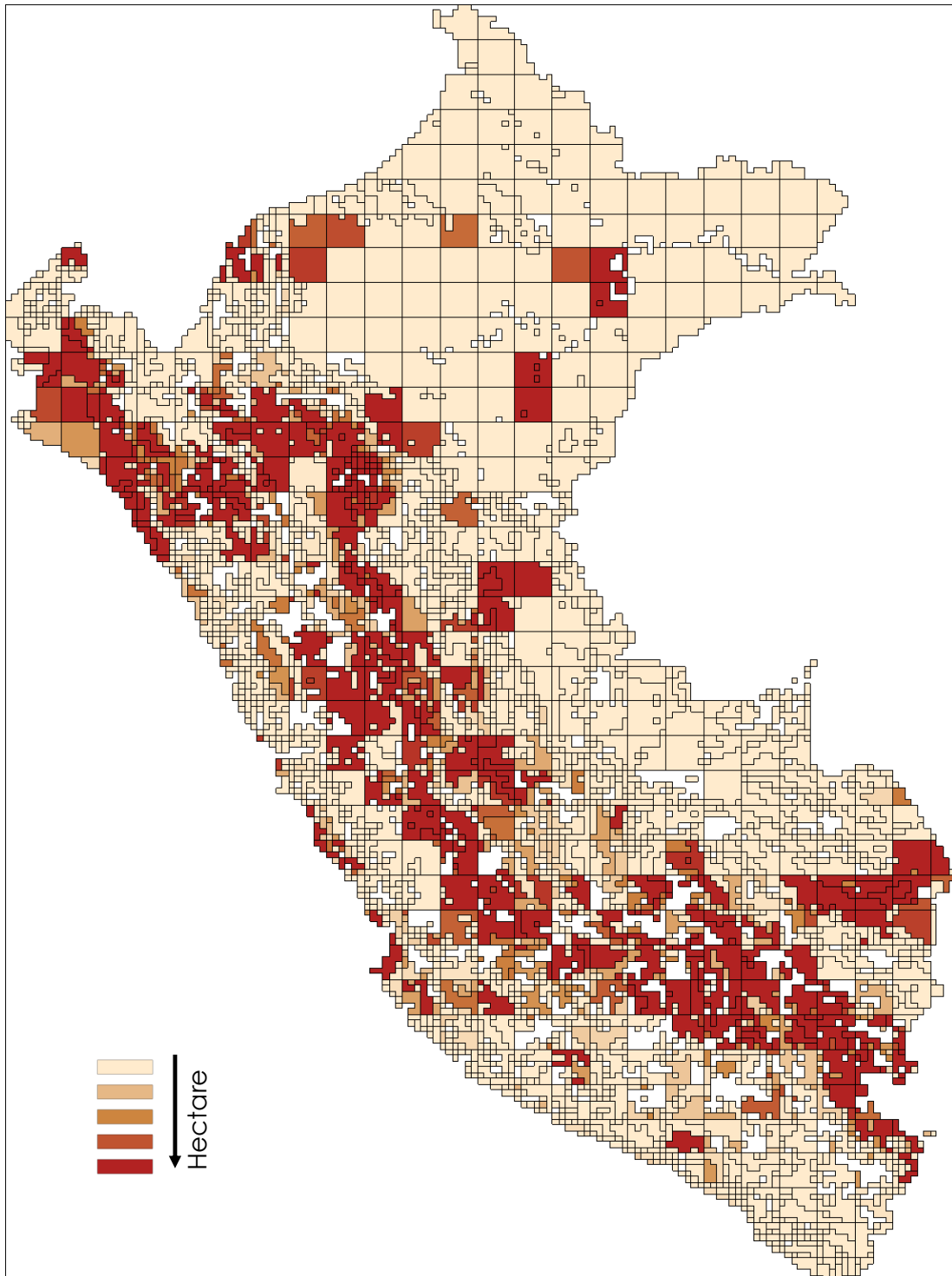


Figure A.10: Cropland adaptation with Side benefit LEVEL 3.

Acknowledgments

This master thesis would not have been possible without the help of numerous people. First, I would like to thank my supervisors, Prof. Johanna, who always helped in word, her lightful ideas, and suggestions made this thesis possible. I highly appreciated having the opportunity to her wisdom guiding me through this journey. My enormous thanks also go to Prof. Uwe. I would not be able to design the adaptation proposal without his guidance. Also, thanks for the patience and support with GAMS and all the coding required. His expertise was indispensable for this part of the analysis. I am also very grateful to SICSS, during this time I got to experience the best two years of my life learning, traveling, discussing, enjoying. I cannot find words to describe what this program mean to me. Thanks, Dr. Ingo, Sebastian and Katja, who were always there to guide and support me. I would also like to thank my mom and dad, who are the major reason for my life, even an ocean could not break us apart. Last but not least, my beloved Pucara, my country, and my friends, the ones here and also in Peru, who happen to believe more in me than I could possibly do.

Declaration of Academic Integrity

”Hiermit versichere ich an Eides statt, dass ich die vorliegende Arbeit im Studiengang Integrated Climate System Sciences selbstständig verfasst und keine anderen als die angegebenen Hilfsmittel – insbesondere keine im Quellenverzeichnis nicht benannten Internet-Quellen – benutzt habe. Alle Stellen, die wörtlich oder sinngemäß aus Veröffentlichungen entnommen wurden, sind als solche kenntlich gemacht. Ich versichere weiterhin, dass ich die Arbeit vorher nicht in einem anderen Prüfungsverfahren eingereicht habe und die eingereichte schriftliche Fassung der auf dem elektronischen Speichermedium entspricht.“

”Hereby I assure on oath that I have independently written the present thesis in the study program Integrated Climate System Sciences and have not used other than the specified resources - in particular no sources not named in the source list. All passages that have been taken literally or analogously from publications are identified as such. I further assure that I have not previously submitted the work in another examination procedure and that the submitted written version corresponds to that on the electronic storage medium.”

Ort, Datum

Unterschrift